Journal of Cellular Physiology

Cells of Extraembryonic Mesodermal Origin Confer Human Dystrophin in the Mdx Model of Duchenne Muscular Dystrophy

YAYOI KAWAMICHI,[1,2,3] CHANG-HAO CUI,[1] MASASHI TOYODA,[1] HATSUNE MAKINO,[1] AKANE HORIE,[1] YORIKO TAKAHASHI,[1] KENJI MATSUMOTO,[4] HIROHISA SAITO,[4] HIROAKI OHTA,[2] KAYOKO SAITO,[3] AND AKIHIRO UMEZAWA[1]*

[1]*Department of Reproductive Biology, National Institute for Child Health and Development, Tokyo, Japan*

[2]*Department of Obstetrics and Gynecology, Tokyo Women's Medical University, Tokyo, Japan*

[3]*Institute of Medical Genetics, Tokyo Women's Medical University, Tokyo, Japan*

[4]*Department of Allergy and Immunology, National Institute for Child Health and Development, Tokyo, Japan*

Duchenne muscular dystrophy is an X-linked recessive genetic disease characterized by severe skeletal muscular degeneration. The placenta is considered to be a promising candidate cell source for cellular therapeutics because it contains a large number of cells and heterogenous cell populations with myogenic potentials. We analyzed the myogenic potential of cells obtained from six parts of the placenta, that is, umbilical cord, amniotic epithelium, amniotic mesoderm, chorionic plate, villous chorion, and decidua basalis. In vitro cells derived from amniotic mesoderm, chorionic plate, and villous chorion efficiently transdifferentiate into myotubes. In addition, in vivo implantation of placenta-derived cells into dystrophic muscles of immunodeficient mdx mice restored sarcolemmal expression of human dystrophin. Differential contribution to myogenesis in this study may be attributed to placental portion-dependent default cell state. Molecular taxonomic characterization of placenta-derived maternal and fetal cells in vitro will help determine the feasibility of cell-based therapy.

J. Cell. Physiol. 223: 695–702, 2010.

The human placenta is a large discoid organ with a diameter of around 20 cm and a weight of approximately 500 g. It contains a large number of cells possessing a wide range of phenotypes and potentials (Cunningham and Williams, 2005; Sadler and Langman, 2006). The functions of the placenta are (a) exchange of metabolic and gaseous products between maternal and fetal bloodstreams and (b) production of hormones, such as progesterone, estradiol, estrogen, and human chorionic gonadotrophin. The placenta consists of the following two components: (a) a fetal portion, derived from the amnion, the chorionic plate (CP), the smooth chorion (chorion laeve (SC)), and the villous chorion (chorion frondosum (VC)) and (b) a maternal portion, derived from the decidua basalis (DB). The amnion, the inner layer, consists of a small amount of connective tissue (amniotic mesoderm (AM)) covered with a cuboidal epithelium (amniotic epithelium (AE)). The amniogenesis is rather complicated, the AM being extraembryonic whereas the AE is from the inner cell mass/embryoblast. The chorion, the outer layer of the amnion, is classified into VC, SC, and CP. The embryonic and abembryonic portions are called villous and SC, respectively. The VC is made of growing and expanding villi, while the CP and SC are made of degenerated villi. The DB, originating from the endometrium, is composed of glandular epithelial cells and stromal (mesenchymal) cells with decidual change. The umbilical cord (UC) that attaches a fetus to the placenta develops from the body stalk of the embryo and contains blood vessels and Wharton jelly, surrounded by the amnion. Each part of the placenta has recently been a candidate cell source for cell-based therapies because of the variety of cell types that become available (Fukuchi et al., 2004; Portmann-Lanz et al., 2006).

One currently untreatable disease which may benefit from cell-based therapy using placenta-derived cells is Duchenne muscular dystrophy (DMD). DMD is an X-linked recessive genetic disease characterized by severe skeletal muscle degeneration. It is caused by a deficiency in dystrophin that is associated with a large oligomeric complex of glycoproteins which provide linkage to the extracellular membrane (Ervasti and Campbell, 1991). The absence of dystrophin results in destabilization of the extracellular membrane–sarcolemma–cytoskeleton architecture, making muscle fibers susceptible to contraction-associated mechanical stress and degeneration. In the first phase of the disease, new muscle fibers are formed by satellite cells. After depletion of the satellite cell pool in

Yayoi Kawamichi, Chang-Hao Cui, and Masashi Toyoda contributed equally to this work.

Additional Supporting Information may be found in the online version of this article.

Contract grant sponsor: Ministry of Health, Labour and Welfare (Nervous and Mental Disorders);
Contract grant number: 18A-1, 19A-7 and 20B-13.
Contract grant sponsor: Japan Health Sciences Foundation;
Contract grant number: KHD1026.
Contract grant sponsor: Ministry of Health, Labour and Welfare (Child Health and Development);
Contract grant number: 21A-3.

*Correspondence to: Akihiro Umezawa, National Institute for Child Health and Development, 2-10-1, Okura, Setagaya, Tokyo 157-8535, Japan. E-mail: umezawa@1985.jukuin.keio.ac.jp

Received 25 August 2009; Accepted 22 December 2009

Published online in Wiley InterScience (www.interscience.wiley.com.), 16 February 2010.
DOI: 10.1002/jcp.22076

childhood, skeletal muscles degenerate progressively and irreversibly and are replaced by fibrotic tissue (Cossu and Mavilio, 2000). No effective therapeutic approaches for muscular dystrophy currently exist; thus, cell-based therapy, in addition to gene therapy (Harper et al., 2002), exon skipping therapy (Matsuo et al., 1991), and read-through therapy by aminoglycoside (Barton-Davis et al., 1999) remain promising treatment options.

Myoblasts represent the natural first choice in cellular therapeutics for skeletal muscle because of their intrinsic myogenic commitment (Grounds et al., 2002). However, myoblasts recovered from muscular biopsies are poorly expandable in vitro and rapidly undergo senescence (Cossu and Mavilio, 2000). Intramuscular allotransplantation of normal muscle precursor cells can induce expression of donor-derived dystrophin in skeletal muscles of patients with DMD (Skuk et al., 2006). However, it is difficult to perform transplantation of muscle precursor cells due to a limited number of donor cells. An alternative source of muscle progenitor cells is therefore desirable. Cells with a myogenic potential are present in many tissues, including bone marrow (Ferrari et al., 1998; Dezawa et al., 2005), UC blood (Gang et al., 2004), adipose tissue (Rodriguez et al., 2005; Di Rocco et al., 2006), and endometrium and menstrual blood (Cui et al., 2007), and all these cells readily form skeletal muscle in culture.

There has, as yet, been no systematic analysis of the distribution of placenta-derived stem cells which have myogenic differentiation potential. Therefore, we characterized each placenta-derived cell in vitro, via a taxonomic approach using global gene expression profiles, and investigated which part of the placenta is the most useful source of stem cells with a myogenic potential that might prove useful for possible future cell-based therapy of DMD.

Materials and Methods

Isolation of human placental tissues

Ethical approval for tissue collection was granted by the Institutional Review Board of the National Institute for Child Health and Development, Japan. Written informed consent was obtained before the sample collection. Human placental samples were collected from normal full-term pregnancies. All of the placentas were processed within 24 h of collection and washed extensively with phosphate-buffered saline (PBS). After peeling off the amnion, the placenta was separated into three parts, that is, CP, VC, and DB. To isolate cells from the UC, the middle part was used, after excluding the edge of the placenta and the tissue close to the fetal navel. The amnion and the SC were manually separated. Amniotic mesodermal cells were manually scraped from the AE. After each placental part was minced using scissors, minced AM was re-suspended in MSCGM (Cambrex Bio Science, Walkersville, MD). We did not calculate the cell numbers at the start of cultivation because the tissue was chopped up mechanically by hand. The placenta-derived cells were maintained at 37°C in a humidified atmosphere containing 5% CO_2 and allowed to attach for 48 h. Non-adherent cells were removed and the medium was changed twice a week. At 70–80% confluence, the cells were harvested with trypsin (0.25%) and 1 mM EDTA (0.02%) in PBS (1:1, v/v) and plated to new dishes. Primary culture cells were used, except for the differentiation analysis. Cells were processed from 45 placentas, and primary cultures from 10 placentas were used for this study.

Flow cytometric analysis

Flow cytometric analysis was performed as previously described (Terai et al., 2005). Briefly, cells were incubated with primary antibodies or isotype-matched control antibodies, followed by additional treatment with the immunofluorescent secondary antibodies. Cells were analyzed on an EPICS ALTRA analyzer (Beckman Coulter, Fullerton, CA). Antibodies against human CD13, CD14, CD29, CD34, CD44, CD45, CD55, CD59, CD73, CD90, CD105, CD166, HLA-ABC, and HLA-DR were purchased from Beckman Coulter, Immunotech (Marseille, France), Cytotech (Hellebaek, Denmark), and BD Biosciences Pharmingen (San Diego, CA).

In vitro myogenesis

In vitro myogenic analysis was performed as previously described (Cui et al., 2007). Briefly, placenta-derived cells were seeded onto 60-mm collagen I-coated cell culture dishes (BD Biocoat™) at a density of 1×10^4/ml in growth medium (Dulbecco's modified Eagle's medium (DMEM), supplemented with 20% fetal bovine serum (FBS)). Forty-eight hours after seeding onto collagen I-coated dishes, the cells were treated with 5 μm 5-azacytidine for 24 h. Cell cultures were then maintained in differentiation medium (DMEM, supplemented with 2% horse serum). The differentiation medium was changed twice a week until the experiment was terminated.

Reverse transcriptase-polymerase chain reaction analysis (RT-PCR) of placenta-derived cells

RT-PCR analysis was performed as previously described (Cui et al., 2007). Briefly, RT-PCR of MyoD, Myf5, myogenin, myosin heavy chain-IIx/d (MyHC-IIx/d), desmin, and dystrophin was performed with 2 μg of total RNA. The sequences of PCR primers that amplify human but not mouse genes are listed in Supplementary Table 1. PCR was performed for 30 cycles, with each cycle consisting of 94°C for 30 sec, 60°C or 65°C for 30 sec, and 72°C for 20 sec, with additional 10-min incubation at 72°C after completion of the last cycle.

Fusion assay in vitro

Placenta-derived cells (2,500/cm^2) were co-cultured with C2C12 myoblasts (2,500/cm^2) for 2 days in DMEM supplemented with 10% FBS, and then cultured for seven additional days in DMEM with 2% horse serum to promote myotube formation. C2C12 myoblast cells were supplied by RIKEN Cell Bank (The Institute of Physical and Chemical Research, Japan). The cultures were fixed in 4% paraformaldehyde (PFA) and stained with a mouse anti-human nuclei IgG1 monoclonal antibody (clone 235-1, Millipore, Billerica, MA) and a mouse anti-myosin heavy chain IgG2b monoclonal antibody (MF-20, Developmental Studies Hybridoma Bank, University of Iowa, IA). The cells were visualized with appropriate Alexa-fluor-conjugated goat anti-mouse IgG1 and IgG2b secondary antibodies (Molecular Probes, Eugene, OR). Total cell nuclei were stained with 4′, 6-diamidino-2-phenylindole (DAPI). To assess the ability of placenta-derived cells to fuse with C2C12 cells, we calculated the percentage of myotubes containing one or more human nuclei in the total myotube as a fusion index.

In vivo cell implantation

The cells (2×10^7) were suspended in PBS, in a total volume of 100 μl, and directly injected into the right tibialis anterior muscle of 6- to 8-week-old mdx/mdx scid/scid (mdx-scid) mice. The mice were euthanized 4 weeks after cell implantation, and the right tibialis anterior muscle was analyzed for human dystrophin by immunohistochemistry.

Immunohistochemical and immunocytochemical analysis

Immunohistochemical and immunocytochemical analyses were performed as previously described (Mori et al., 2005). Briefly, the sections were incubated with a mouse anti-human dystrophin IgG2a monoclonal antibody (NCL-DYS3, Novocastra, UK), and then incubated with horseradish peroxidase-conjugated rabbit anti-mouse immunoglobulin. Staining was developed using a solution containing diaminobenzidine and H_2O_2. Slides were

counterstained with hematoxylin. In the cases of fluorescence, frozen sections fixed with 4% PFA were used. The anti-human dystrophin monoclonal antibody, anti-human nuclei mouse monoclonal antibody, anti-α-sarcoglycan rabbit IgG polyclonal antibody (H-82, Santa Cruz Biotechnology, Santa Cruz, CA) or anti-laminin 2α rat IgG monoclonal antibody (4H8-2, Sigma–Aldrich, St. Louis, MO) was used as the initial antibody, and goat anti-mouse IgG2a conjugated with Alexa Fluor 546, goat anti-mouse IgG1 antibody conjugated with Alexa Fluor 488, goat anti-rabbit IgG conjugated with Alexa Fluor 635, or goat anti-rat IgG conjugated with Alexa Fluor 488 was used as a second antibody. The anti-myogenin mouse monoclonal antibody (F5D, BD Pharmingen, San Diego, CA) was used for immunocytochemistry. As a methodological control, the primary antibody was omitted. In the cases of fluorescence, the slides were incubated with Alexa Fluor 546-conjugated goat anti-mouse IgG antibody.

GeneChip expression analysis

Human genome-wide gene expression was examined with the Human Genome U133 Plus 2.0 Array (GeneChip; Affymetrix, Inc., Santa Clara, CA), which contains the oligonucleotide probe set for more than 47,000 transcripts and variants, including approximately 40,000 well-characterized human genes and expressed sequence tags (ESTs). Total RNA was prepared from samples using the RNeasy Kit (Qiagen, Hilden, Germany), according to the manufacturer's instructions. The purity of RNA was assessed on the Agilent Bioanalyser 2100. Double-stranded cDNA was synthesized from DNase-treated total RNA, and the cDNA was subjected to in vitro transcription in the presence of biotinylated nucleoside triphosphates using the Enzo BioArray HighYield RNA Transcript Labeling Kit (Enzo Life Sciences, Inc., Farmingdale, NY) according to the manufacturer's protocol. The biotinylated cRNA was hybridized with a probe array for 16 h at 45°C, and the hybridized biotinylated cRNA was stained with streptavidin–PE (query 6) and scanned with a Hewlett-Packard Gene Array Scanner (Palo Alto, CA). The fluorescence intensity of each probe was quantified using the GeneChip Analysis Suite 5.0 computer program (Affymetrix) and Robust Multi-array Average (RMA) model (Bolstad et al., 2003; Irizarry et al., 2003a,b). To normalize the variations in staining intensity among chips, the "average difference" values for all genes on a given chip were divided by the median value for expression of all genes on the chip. To eliminate genes containing only a background signal, genes were selected only if the raw values of the "average difference" were more than 200, and if the expression of the gene was judged to be "present" by the GeneChip Operating Software version 1.4 (Affymetrix).

Hierarchical clustering and principal component analysis (PCA)

The hierarchical clustering and PCA techniques classify data by similarity of expression pattern using NIA Array Analysis and TIGR Mev (http://lgsun.grc.nia.nih.gov/ANOVA/, http://www.tm4.org/mev.html).

Results

Morphology of placenta-derived cells

We collected 45 normal full-term placentas which were then separated into six parts, that is, UC, AE, AM, CP, VC, and DB (Fig. 1). Ten placentas were used for the subsequent experiments. Primary cells from each separated part were successfully cultured. These cultured cells appeared to be two morphologically different groups: small fibroblast-like cells and epithelium-like cells (Fig. 2Aa–g). Cells derived from the UC, AM, CP, VC, and DB showed fibroblast-like morphology. However, AE-derived cells and some DB-derived cells exhibited a small cobblestone-like morphology. We obtained 1×10^6 cells after 3-week cultivation of 1 cm^3 of UC, AM, CP, and VC; and 1×10^6 cells after 4-week cultivation of 1 cm^3 of AE and DB.

Surface marker expression and gene chip analysis

Surface markers of primary culture placenta-derived cells, in the absence of any inductive stimuli, were evaluated by flow cytometric analysis (Fig. 2B, Supplementary Figs. 1–5). The cells in "early" primary culture (with low replication number) exhibited a heterogeneous pattern by flow cytometric analysis as shown in Supplementary Figure 5. The "CP" shows two peaks (61.1% positive and 38.9% negative) for CD29 (Supplementary Fig. 5A), and the "DB" contains cells negative for CD29 (8.0%) (Supplementary Fig. 5B). In contrast, the cells in "late" primary culture (with high replication number) show a homogenous pattern by flow cytometric analysis due to the culture conditions in which mesenchymal cells can predominantly proliferate. UC-, AE-, AM-, CP-, VC-, and DB-derived cells were positive for CD13, CD29, CD44, CD55, CD59, CD73, CD90, CD105, and CD166. Placenta-derived cells expressed neither hematopoietic lineage markers, such as CD34, nor monocyte-macrophage antigens, such as CD14 (a marker for macrophage and dendritic cells), or CD45 (leukocyte common antigen). The lack of expression of CD14, CD34, or CD45 suggests that all cells cultured in our experimental setting are depleted of hematopoietic cells. The cell population was positive for HLA-ABC, but not for HLA-DR. Among the placenta-derived cells, that is, UC-, AM-, AE-, CP-, VC-, and DB-derived cells, no significant difference was observed in the expression of mesenchymal stem cell markers, suggesting that the cells are of mesenchymal origin or stromal origin.

To clarify the specific gene expression profile of cells derived from each portion of the placenta, we compared the expression levels using Affymetrix GeneChip oligonucleotide arrays. RNAs were isolated from primary cultured cells of the placenta. The gene expression profile reported in this article has been deposited in the gene Expression Omnibus (GEO) database (http://www.ncbi.nlm.gov/geo: accession no. GSM289889-289894). We performed PCA to determine whether it is possible to discriminate cells of one part from cells of other parts in two-dimensional expression space. PCA, using all probes and 1,087 probes which were annotated with the "transcription factor," revealed that the DB-derived cells are categorized into a distinct group. Statistical analysis revealed that the DB-derived cells significantly express genes for *FOXL2*, *HOP*, *HOXD10*, *HOXD11*, and *HOXA5*. We thus analyzed the *HOX* genes by hierarchical clustering and PCA, since the cells are well categorized, especially based on the *HOX* gene family, and identified three clusters (Fig. 2C,D). Determination of cell specification via gene chip analysis revealed that the each placental cell has a distinct expression pattern of the *HOX* gene family: (a) AE- and AM-derived cells preferentially express the *HOX B* genes, such as *HOX B2*, *B6*, *B7*, and *B8*; (b) DB-derived cells express the *HOX D* genes, such as *D3*, *D4*, *D8*, *D9*, *D10*, and *D11*; (c) the others express the *HOX A* genes, *HOXA13* and *A3*.

In vitro induction of myogenic differentiation

Each distinct part of the placenta has recently been viewed as a candidate source of material for cell-based therapies. We examined, both in vitro and in vivo, whether the placenta-derived cells have a myogenic potential. Of the 54,675 genes represented on the GeneChip, skeletal muscle-specific genes such as the phospholamban, myozenin, dystrobrevin, and myosin heavy chain were expressed in cells derived from VC and the CP. Expression of these muscle-specific genes in these cells led us to hypothesize that these cells are capable of differentiating into myocytes. To prove this, cells from each part of the placenta were exposed to 5-azacytidine for 24 h and then

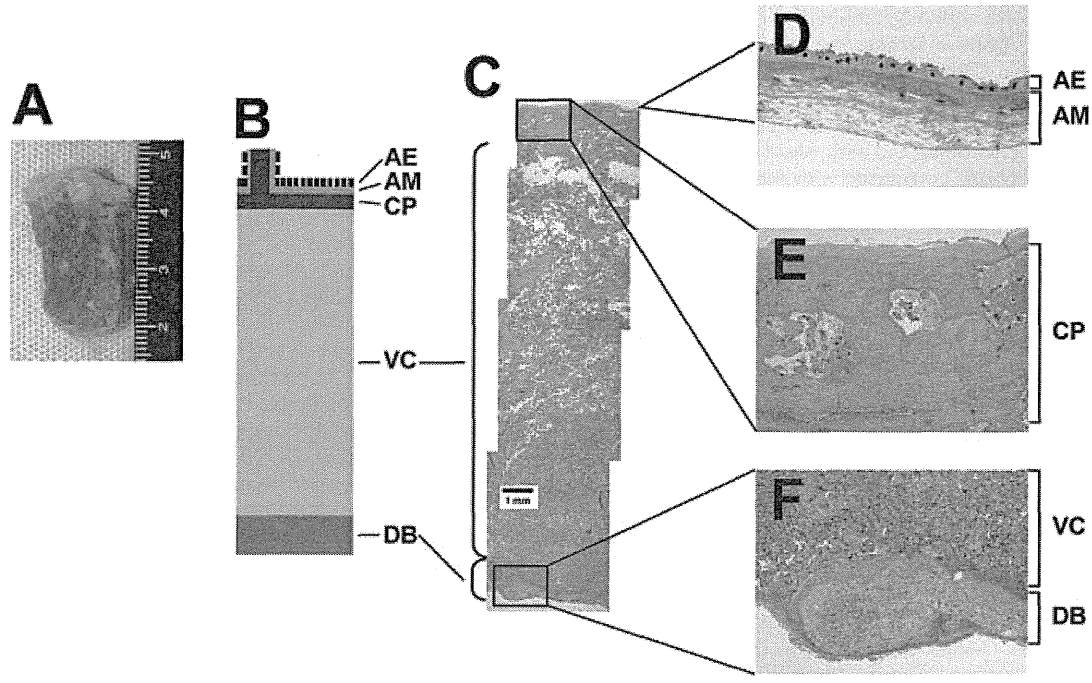

Fig. 1. Placenta-derived cells from each portion. Macroscopy (A) and histology (B,C) of amnion (D), chorionic plate (E), villous chorion, and decidua basalis (F). AE, amniotic epithelium; AM, amniotic mesoderm; CP, chorionic plate; VC, villous chorion; DB, decidua basalis.

cultured in DMEM supplemented with 2% horse serum for 3 weeks. Myogenic differentiation of the cells was analyzed by evaluating the expression of MyoD, Myf5, myogenin, MyHC-IIx/d, and desmin by RT-PCR and immunocytochemistry (Fig. 3). MyoD is constitutively expressed in amniotic mesodermal cells but decreased to no measurable level at day 3 and thereafter (Fig. 3A). In the case of the CP and VC, MyoD expression is detected at 3 weeks. Expression of genes encoding MyoD, Myf5, myogenin, and MyHC-IIx/d was under a detectable level in cells derived from UC, AE, and DB even after myogenic induction. MyHC-IIx/d, a structural gene, started to be expressed at the middle of differentiation in amniotic mesodermal cells and at the late stage in CP-derived cells. Desmin was expressed in cells derived from AM, UC, CP, AE, and DB throughout differentiation. In the cells derived from AM and CP, dystrophin expression increased after myogenic induction (Fig. 3B). Immunocytochemical analysis revealed that CP-derived cells became positive for MyHC-IIx/d, α-sarcoglycan, and myogenin after cultivation with 2% horse serum for 21 days (Fig. 3C–E). However, without any treatment, the cells did not show myotube-like morphology (Fig. 3Cc). C2C12 myoblasts were used for a positive control of immunocytochemistry (Supplementary Fig. 6). Placenta-derived cells from each portion exhibit different capabilities for proliferation and myogenesis in vitro (Fig. 3F).

Detection of human placental cell contribution to myotubes in an in vitro myogenesis model

To simulate in vivo phenomena, human placental cells were co-cultured in vitro with murine C2C12 myoblasts for 2 days under proliferative conditions and then switched to differentiation conditions for an additional 7 days. Multinucleated myotubes were formed after co-culturing with C2C12 cells (Fig. 4). Myosin heavy chain and human nuclei were unequivocally identified by staining with MF20 and an antibody to human nuclei, while the numerous mouse nuclei present in this field, as shown by DAPI staining, are negative. The frequency of fusion between placenta-derived cells and C2C12 myotube depends on the cell type: cells derived from CP and DB exhibited high frequencies of fusion, whereas cells derived from AE and UC induced low-level fusion to C2C12 myocytes. No multinucleated cells were formed without co-cultivation.

Expression of human dystrophin by cell implantation in the mdx-scid mouse

To investigate whether placenta-derived cells can generate muscle tissue in vivo, cells (2×10^7) without any treatment or induction were implanted directly into the right anterior tibialis muscles of mdx-scid mice. PBS without cells was injected into the left anterior tibialis muscle as a control. After 4 weeks, myofibers in the muscle tissues injected with amniotic mesodermal cells expressed human dystrophin and laminin (Fig. 5). Dystrophin was not detected in the muscle of mdx-scid mice without cell implantation because the antibody to dystrophin used in this study is human-specific, implying that dystrophin is transcribed from dystrophin genes of human donor cells but not from reversion of dystrophied myocytes in mdx-scid mice.

Discussion

Differential myogenic potential of cultured cells from each part of the placenta

The placenta includes cells of maternal and fetal origin. Although most placenta-derived cells are of extraembryonic origin, AE-derived cells are from the epiblast/inner cell mass of the blastocyst (Cunningham and Williams, 2005; Sadler and Langman, 2006). The aim of this study was to determine the intrinsic differentiation potential of cells from six parts of the

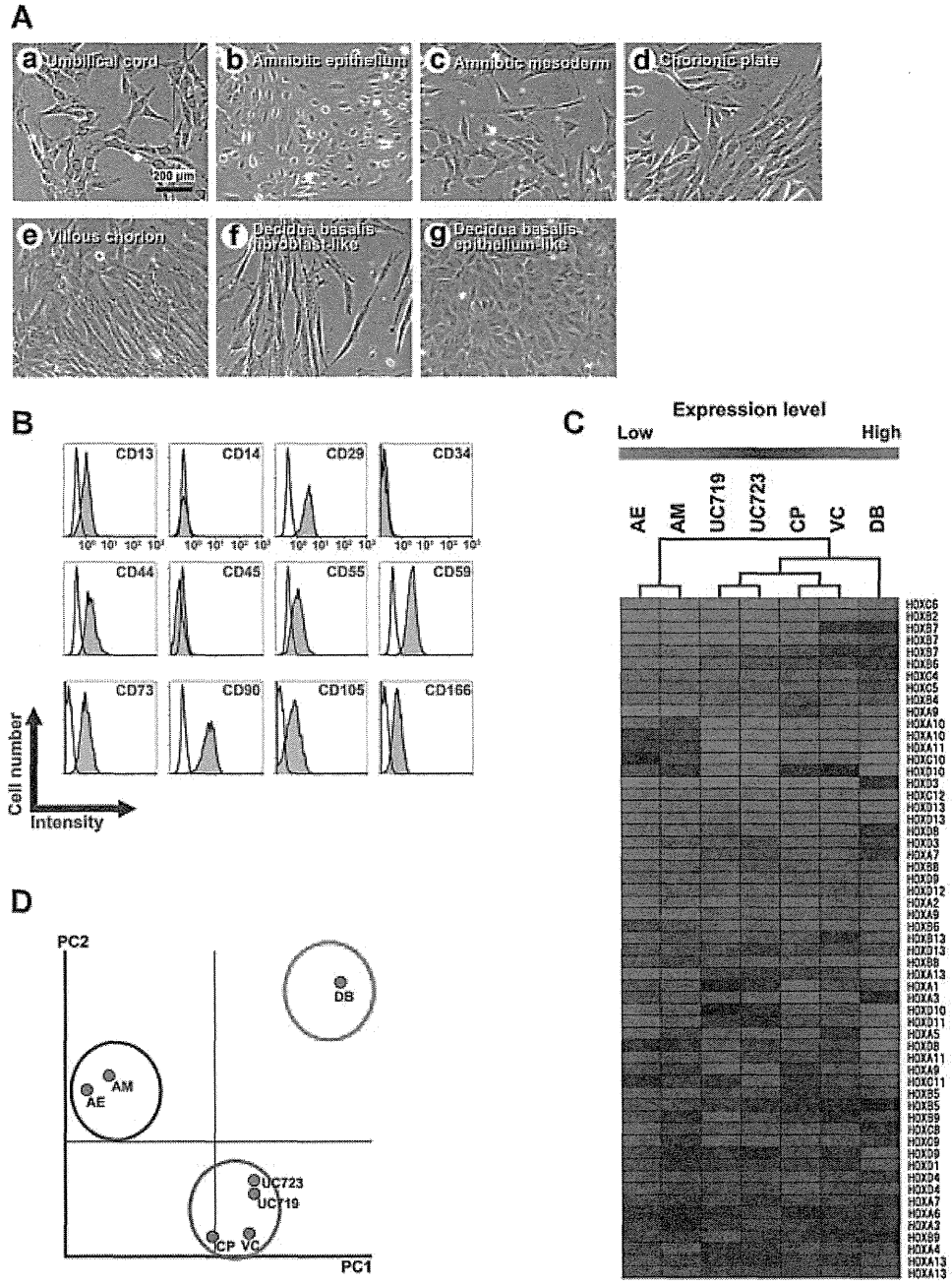

Fig. 2. Morphology of placenta-derived cells and flow cytometric analysis of amniotic mesoderm-derived cells. A: Photomicrographs of cells from umbilical cord-derived cells (a), amniotic epithelial cells (b), amniotic mesodermal cells (c), chorionic plate-derived cells (d), villous chorion-derived cells (e), decidua basalis-derived cells (f: fibroblast-like, g: epithelial cell-like) from primary culture. Amniotic epithelial cells (b) and decidua basalis-derived cells (g) showed an epithelial cell-like (cobblestone-like) morphology, while the others (a,c,d,e,f) showed a fibroblast-like morphology. Scale bars: 200 μm. B: Flow cytometric analysis of amniotic mesoderm-derived cells in primary culture (with high replication number) in the absence of any inductive stimuli. Non-shaded and shaded areas indicated reactivity of antibodies for isotype controls and that of antibodies for cell surface markers, respectively. C: Hierarchical clustering analysis and heat map analysis of *HOX* gene expression in cells derived from umbilical cord (UC719 and UC723), amniotic epithelium (AE), amniotic mesoderm, (AM), chorionic plate (CP), villous chorion (VC), decidua basalis (DB), using "TIGR MeV." D: PCA revealing general trends of *HOX* gene expression.

placenta, that is, UC, AE, AM, CP, VC, and DB. The myogenic potential of cells from the AM, CP, and VC proved much greater than expected, and this higher myogenic differentiation ratio can be a reflection of the intrinsic cellular potential of extraembryonic mesodermal cells. Lack of myogenic potential in AE-derived cells is envisaged because the cells are of extraembryonic ectodermal origin and cuboidal in morphology.

Despite our findings, amniotic epithelial cells have been reported to have the potential to differentiate to all three germ layer cells, including myocytes, after in vitro sphere formation (Miki et al., 2005). Amniotic epithelial cells formed neither spheres nor viable supernatant cells in our experimental settings, but displayed a cobblestone appearance with an epithelial phenotype. Cells obtained from AE, we believe,

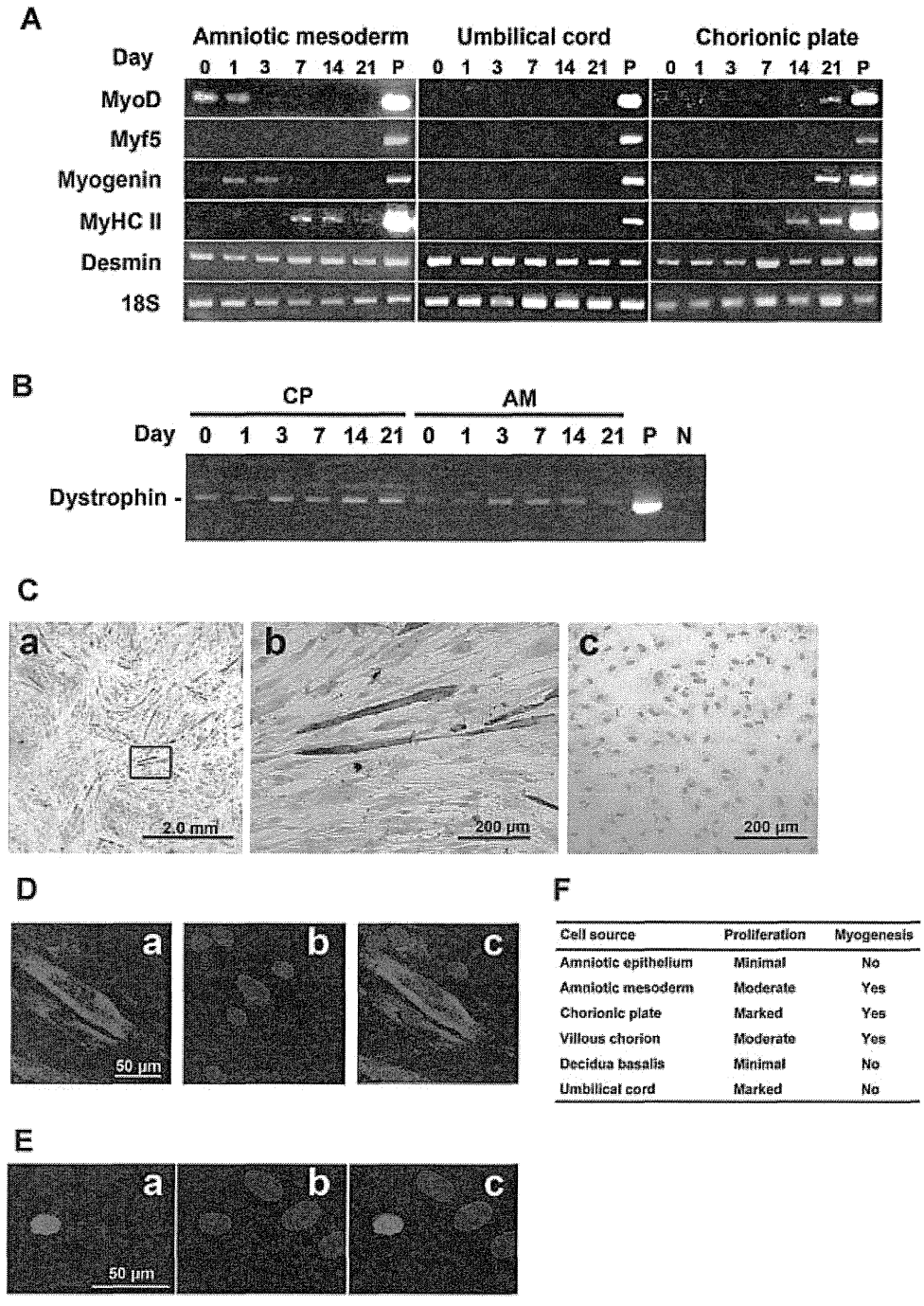

Cell source	Proliferation	Myogenesis
Amniotic epithelium	Minimal	No
Amniotic mesoderm	Moderate	Yes
Chorionic plate	Marked	Yes
Villous chorion	Moderate	Yes
Decidua basalis	Minimal	No
Umbilical cord	Marked	No

Fig. 3. Expression of muscle-specific genes during differentiation of placenta-derived cells. A: RT-PCR analysis of human MyoD, Myf5, myogenin, myosin heavy chain type IIx/d (MyHC-IIx/d), desmin, and 18S cDNA (from top to bottom). Amniotic mesodermal cells, umbilical cord-derived cells, and chorionic plate-derived cells were exposed to 5 μM 5-azacytidine for 24 h and then subsequently cultured in DMEM supplemented with 2% HS for 21 days. RNAs from human muscle serve as a positive (P) control. Only the 18S PCR primer used as a positive control reacted with the human and murine cDNA. B: RT-PCR analysis of human dystrophin in chorionic plate (CP) and amniotic mesodermal cells (AM). The muscle-specific isoform (Dp427m) was amplified. RNAs from human muscle serve as a positive (P) control. C: Immunocytochemistry of skeletal myosin heavy chain in chorionic plate-derived cells after myogenic induction (a,b) or no induction (c). Scale bars: (a) 2.0 mm, (b,c) 200 μm. D: Immunocytochemistry of α-sarcoglycan. a: α-sarcoglycan; b: DAPI staining; c: "merge" of a and b. Scale bars: 50 μm. E: Immunocytochemistry of myogenin. a: myogenin; b: DAPI staining; c: "merge" of a and b. Scale bars: 50 μm. F: Cell site origin and capability for proliferation and myogenesis.

correspond to previously reported adherent cells with little myogenic activity (Miki et al., 2005). The poor myogenic capability of UC-derived cells was also contrary to our expectation based on prior research (Conconi et al., 2006). It may also be due to intrinsic cell characteristics (or cell mission), and UC-derived cells embedded in Wharton's jelly may be terminally differentiated cells or highly specific cells which produce a matrix for cushioning of the cord.

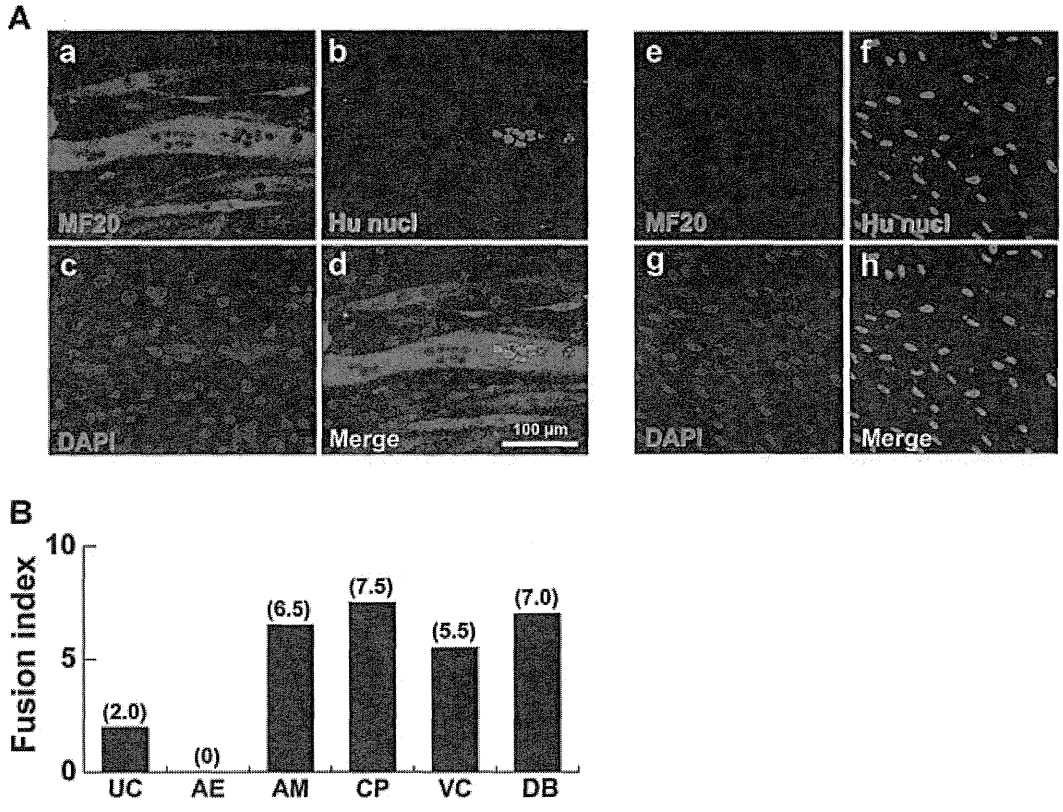

Fig. 4. Detection of human placenta-derived cell contribution to myotubes in an in vitro myogenesis model. The chorionic plate-derived cells were co-cultured with C2C12 myoblasts for 2 days under conditions that favored proliferation. The cultures were then changed to differentiation media for 7 days to induce myogenic fusion. A: Fusion between human chorionic plate-derived cells and murine C2C12 cells. a: human myosin heavy chain molecule (red, MF20); b: human nuclei (HuNucl, green); c: DAPI staining (blue); d: "merge" of a, b, and c. Scale bars: 100 μm. e–h: Human chorionic plate-derived cells without co-culturing. e: human myosin heavy chain molecule (red, MF20); f: human nuclei (HuNucl, green); g: DAPI staining (blue); h: "merge" of e, f, and g. B: Comparison of fusion between each placenta-derived cell and mouse C2C12 myoblasts. Fusion index is shown as number of fused cells per 1,000 cells. UC, umbilical cord; AE, amniotic epithelium; AM, amniotic mesoderm; CP, chorionic plate; VC, villous chorion; DB, decidua basalis.

Taxonomic approach using global gene expression database

In general, cultured cells reflect in vivo characteristics, for example, hematopoietic cells proliferate as a supernatant cell in culture, and epithelial cells exhibit cobblestone appearance at confluence. In contrast, mesenchymal/stromal cells from each part of the placenta, regardless of cell source, show similar appearance in vitro and in vivo, irrespective of their diversity with respect to differentiation and proliferation. The different phenotypes of mesenchymal/stromal cells are maintained even after a series of cell replications and passages, probably by epigenetics, such as genomic methylation and chromatin of cells. The stably transmitted epigenetics in cultured cells reflects a gene expression network and maintains cell identity, and thus each mesenchymal cell is predictable by the results of gene expression with GeneChip analysis. Categorization of the cells may reflect the native functional difference, even after cultivation, and implies that cells from the UC, AE, AM, CP, VC, and DB have a distinct cell identity, in addition to mesenchymal or epithelial phenotypes.

Cell-based therapy for DMD

DMD is a fatal disease for which an effective treatment is still being actively sought. As a novel treatment option, stem cells could be used to replace defective dystrophin and restore the dystrophic muscles. Most placenta-derived cells are either myogenic progenitors or have myogenic potential, and clearly cells with the highest myogenic potential would be beneficial for treatment of dystrophic muscle. Acquisition or recovery of dystrophin expression in dystrophic muscle is attributed to two different mechanisms: (a) myogenic differentiation of implanted or transplanted cells and (b) cell fusion of implanted or transplanted cells with host muscle cells. In this study using placenta-derived cells, our findings, namely that implantation of placenta-derived cells improved the efficiency of muscle regeneration and dystrophin delivery to dystrophic muscle in mice, are explained by both possibilities or the latter possibility (fusion mechanism) alone. Efficient fusion systems of placenta-derived cells with host dystrophic myocytes may contribute substantially to a major advance toward eventual cell-based therapies for muscle injury or chronic muscular disease.

The isolation of tissue-specific stem cells for expansion in vitro and transplantation back into the patient in an allogeneic manner is indeed an ideal strategy, from the viewpoint of industry-based, sustainable supply of large quantities of affordable, quality-controlled cells. In most cases of degenerative diseases and genetic diseases, such as lysosomal storage diseases, it is unlikely that enough unaffected stem cells will be isolated or available in sufficient quantity, necessitating the use of stem cells from suitable, cost-effective allogeneic sources, such as human placenta. The predicted number of AM-derived cells from one placenta of an average size (500 g)

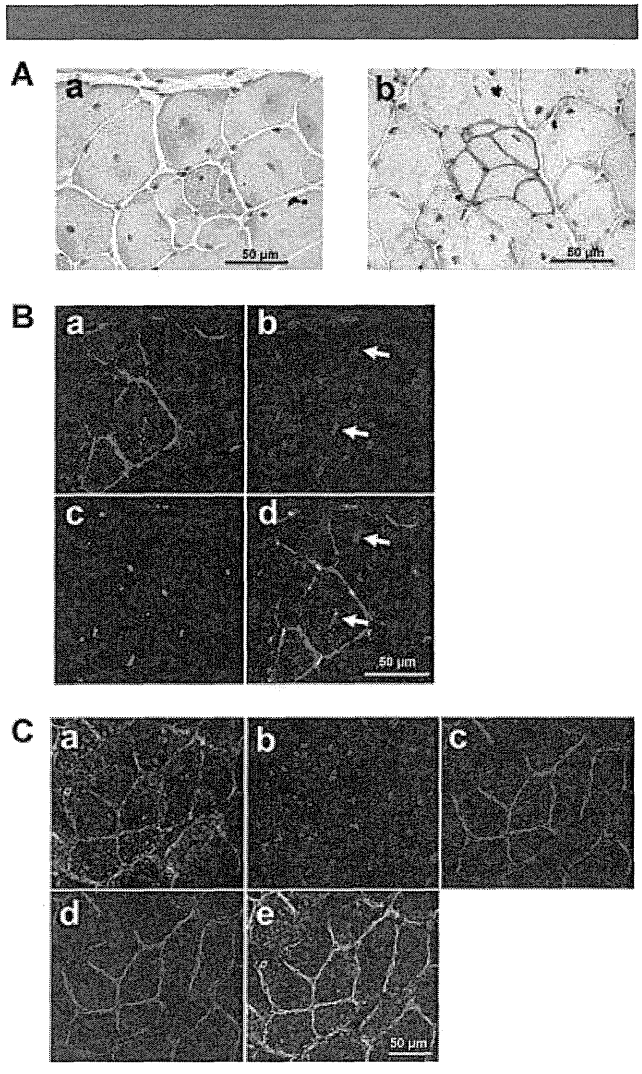

Fig. 5. Conferral of dystrophin to mdx myocytes by human placenta-derived cells. A: Immunohistochemistry using an antibody against human dystrophin on anterior tibialis muscle sections of mdx-scid mice after direct injection of PBS without cells (a: negative control) or amniotic mesoderm-derived cells without any treatment or induction (b) into mdx-scid myofibers. Scale bars: 50 μm. B: Immunohistochemistry analysis on anterior tibialis muscle sections of mdx-scid mice after direct injection of amniotic mesoderm-derived cells without any treatment or induction. Immunohistochemistry revealed the incorporation of implanted cells into newly formed myofibers, which expressed human dystrophin 4 weeks after implantation. Murine nuclei are indicated by arrows. a: human dystrophin molecule (red); b: DAPI staining (blue); c: human nuclei (HuNucl, green); d: "merge" of a, b, and c. Scale bars: 50 μm. C: Immunohistochemistry analysis on anterior tibialis muscle sections of mdx-scid mice after direct injection of amniotic mesoderm-derived cells. a: α-sarcoglycan (yellow); b: DAPI staining (blue); c: laminin (red); d: human dystrophin (green); e: "merge" of a, b, c, and d. Scale bars: 50 μm.

would be approximately 1×10^6 (before ex vivo amplification), possibly reaching 1×10^{11} after cultivation. This may cover 3,000 cm^3 of muscular tissues in cell-based therapy (Skuk et al., 2006). Cells converted into myotubes in vitro at a high frequency after induction, giving rise to large numbers of myofibers expressing human dystrophin when transplanted into BALB/c and mdx mice, thus fulfilling all the criteria required for a successful allogeneic cell therapy for muscular dystrophy. It should also be remembered that currently, implantation of placenta-derived cells in an allogeneic combination requires administration of immunosuppressive drugs, such as FK506 and steroids.

We have established a method for systemic mapping of placental cells with myogenic potential. Cellular dissection and cultivation, coupled with accurate determination of the molecular characteristics of specific cells in the human placenta, opens up significant new possibilities in regenerative medicine. The outcome of this study indicates a potential cell-based treatment for DMD, a lethal human disease for which no effective treatment currently exists.

Acknowledgments

We would like to express our sincere thanks to H. Abe and M. Inoue-Yamazaki for providing expert technical assistance, to K. Saito for her secretarial work, and to A. Crump for reviewing the manuscript.

Literature Cited

Barton-Davis ER, Cordier L, Shoturma DI, Leland SE, Sweeney HL. 1999. Aminoglycoside antibiotics restore dystrophin function to skeletal muscles of mdx mice. J Clin Invest 104:375–381.

Bolstad BM, Irizarry RA, Astrand M, Speed TP. 2003. A comparison of normalization methods for high density oligonucleotide array data based on variance and bias. Bioinformatics 19:185–193.

Conconi MT, Burra P, Di Liddo R, Calore C, Turetta M, Bellini S, Bo P, Nussdorfer GG, Parnigotto PP. 2006. CD105(+) cells from Wharton's jelly show in vitro and in vivo myogenic differentiative potential. Int J Mol Med 18:1089–1096.

Cossu G, Mavilio F. 2000. Myogenic stem cells for the therapy of primary myopathies: Wishful thinking or therapeutic perspective? J Clin Invest 105:1669–1674.

Cui CH, Uyama T, Miyado K, Terai M, Kyo S, Kiyono T, Umezawa A. 2007. Menstrual blood-derived cells confer human dystrophin expression in the murine model of Duchenne muscular dystrophy via cell fusion and myogenic transdifferentiation. Mol Biol Cell 18:1586–1594.

Cunningham FG, Williams JW. 2005. Implantation, embryogenesis, and placenta development. In: Williams obstetrics, 22nd edition. New York: McGraw-Hill Professional. pp 39–90.

Dezawa M, Ishikawa H, Itokazu Y, Yoshihara T, Hoshino M, Takeda S, Ide C, Nabeshima Y. 2005. Bone marrow stromal cells generate muscle cells and repair muscle degeneration. Science 309:314–317.

Di Rocco G, Iachininoto MG, Tritarelli A, Straino S, Zacheo A, Germani A, Crea F, Capogrossi MC. 2006. Myogenic potential of adipose-tissue-derived cells. J Cell Sci 119:2945–2952.

Ervasti JM, Campbell KP. 1991. Membrane organization of the dystrophin-glycoprotein complex. Cell 66:1121–1131.

Ferrari G, Cusella-De Angelis G, Coletta M, Paolucci E, Stornaiuolo A, Cossu G, Mavilio F. 1998. Muscle regeneration by bone marrow-derived myogenic progenitors. Science 279:1528–1530.

Fukuchi Y, Nakajima H, Sugiyama D, Hirose I, Kitamura T, Tsuji K. 2004. Human placenta-derived cells have mesenchymal stem/progenitor cell potential. Stem Cells 22:649–658.

Gang EJ, Jeong JA, Hong SH, Hwang SH, Kim SW, Yang IH, Ahn C, Han H, Kim H. 2004. Skeletal myogenic differentiation of mesenchymal stem cells isolated from human umbilical cord blood. Stem Cells 22:617–624.

Grounds MD, White JD, Rosenthal N, Bogoyevitch MA. 2002. The role of stem cells in skeletal and cardiac muscle repair. J Histochem Cytochem 50:589–610.

Harper SQ, Hauser MA, DelloRusso C, Duan D, Crawford RW, Phelps SF, Harper HA, Robinson AS, Engelhardt JF, Brooks SV, Chamberlain JS. 2002. Modular flexibility of dystrophin: Implications for gene therapy of Duchenne muscular dystrophy. Nat Med 8:253–261.

Irizarry RA, Bolstad BM, Collin F, Cope LM, Hobbs B, Speed TP. 2003a. Summaries of Affymetrix GeneChip probe level data. Nucleic Acids Res 31:e15.

Irizarry RA, Hobbs B, Collin F, Beazer-Barclay YD, Antonellis KJ, Scherf U, Speed TP. 2003b. Exploration, normalization, and summaries of high density oligonucleotide array probe level data. Biostatistics 4:249–264.

Matsuo M, Masumura T, Nishio H, Nakajima T, Kitoh Y, Takumi T, Koga J, Nakamura H. 1991. Exon skipping during splicing of dystrophin mRNA precursor due to an intraexon deletion in the dystrophin gene of Duchenne muscular dystrophy kobe. J Clin Invest 87:2127–2131.

Miki T, Lehmann T, Cai H, Stolz DB, Strom SC. 2005. Stem cell characteristics of amniotic epithelial cells. Stem Cells 23:1549–1559.

Mori T, Kiyono T, Imabayashi H, Takeda Y, Tsuchiya K, Miyoshi S, Makino H, Matsumoto K, Saito H, Ogawa S, Sakamoto M, Hata J, Umezawa A. 2005. Combination of hTERT and bmi-1, E6, or E7 induces prolongation of the life span of bone marrow stromal cells from an elderly donor without affecting their neurogenic potential. Mol Cell Biol 25:5183–5195.

Portmann-Lanz CB, Schoeberlein A, Huber A, Sager R, Malek A, Holzgreve W, Surbek DV. 2006. Placental mesenchymal stem cells as potential autologous graft for pre- and perinatal neuroregeneration. Am J Obstet Gynecol 194:664–673.

Rodriguez AM, Pisani D, Dechesne CA, Turc-Carel C, Kurzenne JY, Wdziekonski B, Villageois A, Bagnis C, Breittmayer JP, Groux H, Ailhaud G, Dani C. 2005. Transplantation of a multipotent cell population from human adipose tissue induces dystrophin expression in the immunocompetent mdx mouse. J Exp Med 201:1397–1405.

Sadler TW, Langman J. 2006. Third month to birth: The fetus and placenta. In: Langman's medical embryology, 10th edition. Philadelphia: Lippincott Williams & Wilkins. pp 89–109.

Skuk D, Goulet M, Roy B, Chapdelaine P, Bouchard JP, Roy R, Dugre FJ, Sylvain M, Lachance JG, Deschenes L, Senay H, Tremblay JP. 2006. Dystrophin expression in muscles of duchenne muscular dystrophy patients after high-density injections of normal myogenic cells. J Neuropathol Exp Neurol 65:371–386.

Terai M, Uyama T, Sugiki T, Li XK, Umezawa A, Kiyono T. 2005. Immortalization of human fetal cells: The life span of umbilical cord blood-derived cells can be prolonged without manipulating p16INK4a/RB braking pathway. Mol Biol Cell 16:1491–1499.

RESEARCH ARTICLE

AMERICAN JOURNAL OF medical genetics PART A

Recessive *RYR1* Mutations in a Patient With Severe Congenital Nemaline Myopathy With Ophthalomoplegia Identified Through Massively Parallel Sequencing

Eri Kondo,[1] Takafumi Nishimura,[2] Tomoki Kosho,[3] Yuji Inaba,[2] Satomi Mitsuhashi,[4] Takefumi Ishida,[2] Atsushi Baba,[2] Kenichi Koike,[2] Ichizo Nishino,[4] Ikuya Nonaka,[4] Toru Furukawa,[5] and Kayoko Saito[1]***

[1]Institute of Medical Genetics, Tokyo Women's Medical University, Tokyo, Japan

[2]Department of Pediatrics, Shinshu University School of Medicine, Matsumoto, Japan

[3]Department of Medical Genetics, Shinshu University School of Medicine, Matsumoto, Japan

[4]Department of Neuromuscular Research, National Institute of Neuroscience, National Center of Neurology and Psychiatry, Kodaira, Tokyo, Japan

[5]Tokyo Women's Medical University Institute for Integrated Medical Sciences, Tokyo, Japan

Received 1 October 2011; Accepted 8 January 2012

Nemaline myopathy (NM) is a group of congenital myopathies, characterized by the presence of distinct rod-like inclusions "nemaline bodies" in the sarcoplasm of skeletal muscle fibers. To date, *ACTA1*, *NEB*, *TPM3*, *TPM2*, *TNNT1*, and *CFL2* have been found to cause NM. We have identified recessive *RYR1* mutations in a patient with severe congenital NM, through high-throughput screening of congenital myopathy/muscular dystrophy-related genes using massively parallel sequencing with target gene capture. The patient manifested fetal akinesia, neonatal severe hypotonia with muscle weakness, respiratory insufficiency, swallowing disturbance, and ophthalomoplegia. Skeletal muscle histology demonstrated nemaline bodies and small type 1 fibers, but without central cores or minicores. Congenital myopathies, a molecularly, histopathologically, and clinically heterogeneous group of disorders are considered to be a good candidate for massively parallel sequencing.

Key words: nemaline myopathy (NM); massively parallel sequencing; the ryanodine receptor type 1 gene (*RYR1*); fetal akinesia; ophthalomoplegia

How to Cite this Article:
Kondo E, Nishimura T, Kosho T, Inaba Y, Mitsuhashi S, Ishida T, Baba A, Koike K, Nishino I, Nonaka I, Furukawa T, Saito K. 2012. Recessive *RYR1* mutations in a patient with severe congenital nemaline myopathy with ophthalomoplegia identified through massively parallel sequencing.
Am J Med Genet Part A 158A:772–778.

INTRODUCTION

Nemaline myopathy (NM) constitutes a group of congenital myopathies, characterized by the presence of distinct rod-like inclusions "nemaline bodies" in the sarcoplasm of skeletal muscle fibers. NM is clinically classified into six forms: severe congenital form, Amish NM, intermediate congenital form, typical congenital form, childhood-onset form, and adult-onset form. Severe congenital NM presents at birth with severe hypotonia and muscle weakness, little spontaneous movement, difficulties in sucking and

Additional supporting information may be found in the online version of this article.

Grant sponsor: Research Committee of Spinal muscular atrophy (SMA); Grant sponsor: Support Center for Women's Health Care Professionals and Researchers; Grant sponsor: Research on Intractable Diseases, Ministry of Health, Labour and Welfare, Japan; Grant sponsor: Ministry of Education, Culture, Sports, Science and Technology in Japan.

Eri Kondo and Takafumi Nishimura contributed equally to this work.

*Correspondence to:
Kayoko Saito, M.D., Ph.D., Institute of Medical Genetics, Tokyo Women's Medical University, 10-22 Kawada-cho, Shinjuku-ku, Tokyo 162-0054, Japan. E-mail: saito@img.twmu.ac.jp
**Correspondence to:
Tomoki Kosho, M.D., Department of Medical Genetics, Shinshu University School of Medicine, 3-1-1 Asahi, Matsumoto 390-8621, Japan. E-mail: ktomoki@shinshu-u.ac.jp

Published online 9 March 2012 in Wiley Online Library (wileyonlinelibrary.com).
DOI 10.1002/ajmg.a.35243

swallowing, gastroesophageal reflux, and respiratory insufficiency. Decreased fetal movements, polyhydramnios, and intrauterine death could occur. Early mortality is common, usually resulting from respiratory insufficiency or aspiration pneumonia, though occasional patients could survive long-term. To date, six genes have been found to cause NM: *ACTA1* (OMIM 102610), *NEB* (OMIM 161650), *TPM3* (OMIM 191030), *TPM2* (OMIM 190990), *TNNT1* (OMIM 191041), and *CFL2* (OMIM 601443) [North and Ryan, 2010]. *ACTA1* mutations are reported to account for roughly half of cases with severe congenital NM [Agrawal et al., 2004].

In this study, we report on a patient with severe congenital NM, characterized clinically by persistent ophthalomoplegia and histologically by small type 1 fibers in addition to nemaline bodies, but without central cores or minicores. Massively parallel sequencing of congenital myopathy/muscular dystrophy-related genes successfully identified compound heterozygous mutations in the ryanodine receptor type 1 gene (*RYR1*) (OMIM 180901).

CLINICAL REPORT

We investigated a now 2-year-old boy, clinically and histologically diagnosed with severe congenital NM. He is the first child of a healthy non-consanguineous Japanese couple with no family history of neuromuscular disorders. The fetal period had been complicated by nuchal translucency, fetal akinesia, and massive polyhydramnios. He was delivered at 35 weeks of gestation by vaginal vacuum extraction, with an Apgar score of 1 at 1 min. His birth weight was 2,048 g (−0.8SD), length 45 cm (−0.2SD), and head circumference 34 cm (+1.3SD). He showed severe generalized hypotonia, muscle weakness, central cyanosis, and bradycardia. After resuscitation with intratracheal intubation for severe apnea, he was admitted to the neonatal intensive care unit. He had a narrow face with facial muscle weakness, a high palate, reduced mouth opening, and mild bilateral blepharoptosis and ophthalmoplegia (Fig. 1a). On an appropriate ventilatory support, severe generalized muscle weakness and hypotonia persisted with a frog-leg posture and poor anti-gravity movements of the limbs (Fig. 1b). Extension of the elbows and knees were mildly limited. Micropenis, hypoplastic scrotum, and bilateral cryptorchidism were present. After tube feeding was started on the second day of birth, chylothorax occurred, requiring temporary intravenous nutrition. Serum creatine kinase and aldolase levels were normal. Nerve conduction studies showed normal velocities, amplitudes, and latencies. Electromyography showed myopathic changes (Fig. 2a).

He showed severe growth retardation in infancy. He had tracheotomy at age 6 months and gastrostomy with Nissen fundoplication at age 1 year. His height and weight caught up to normal ranges (Fig. 2b). From age 1 year, he gradually began moving his upper and lower extremities against gravity and the joint contractures improved, but proximal muscle weakness was still pronounced. He had no difficulties in opening his eyes, but no ocular movement was observed. He showed no swallowing

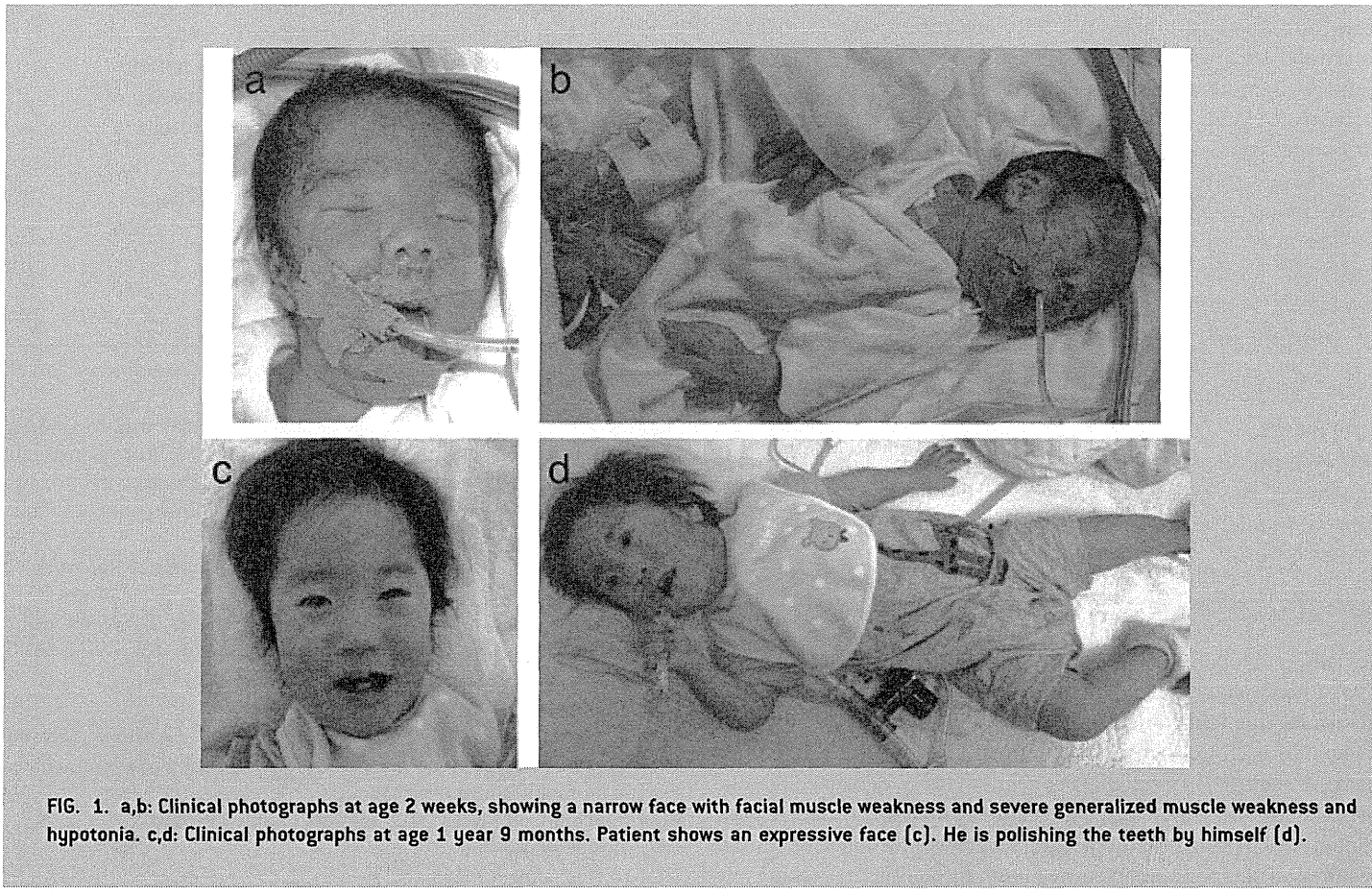

FIG. 1. a,b: Clinical photographs at age 2 weeks, showing a narrow face with facial muscle weakness and severe generalized muscle weakness and hypotonia. c,d: Clinical photographs at age 1 year 9 months. Patient shows an expressive face (c). He is polishing the teeth by himself (d).

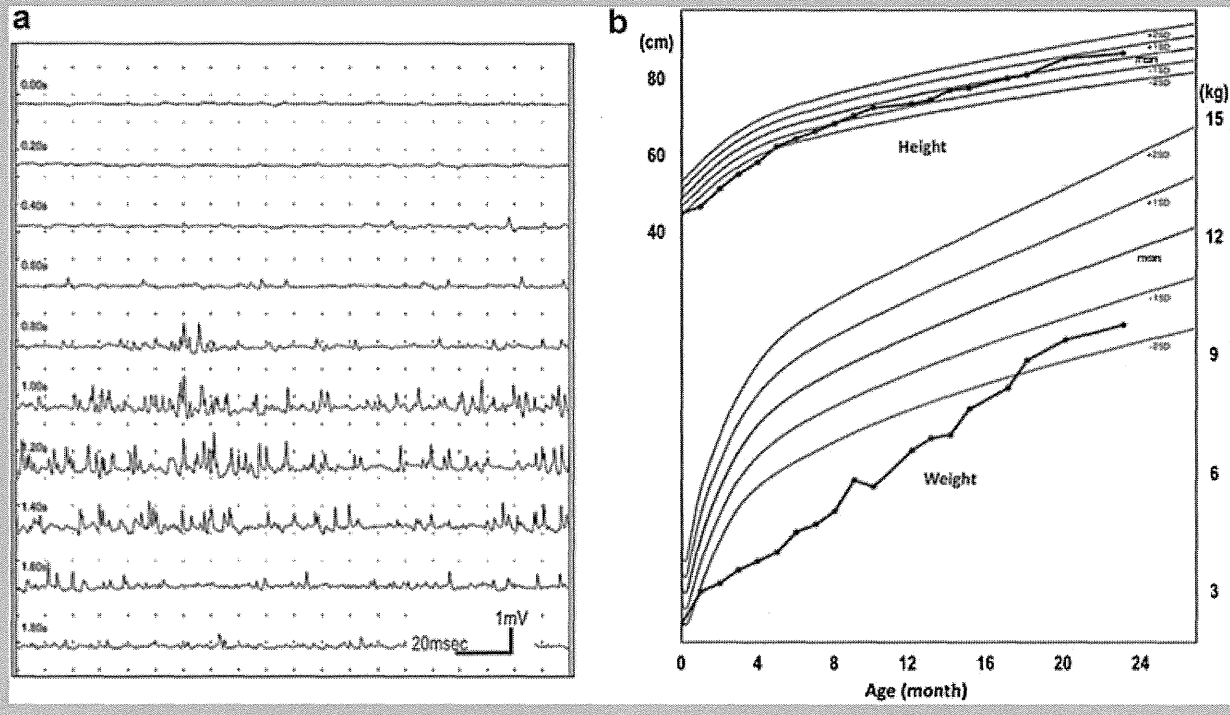

FIG. 2. a: Electromyography at age 2 months showing no abnormal insertion or resting discharges, but lower amplitudes and shorter durations in contraction. b: Growth curve showing both height and weight, delayed in infancy, catching up to normal ranges.

movement. He reached for an object at age 14 months, grasped an object at 16 months, and rolled over at 18 months. Social development was also observed, such as imitating his mother's hand movements at age 14 months and playing "peek-a-boo" at 16 months. When last seen by us at age 1 year and 9 months, he showed an expressive face and an active limb movement (Fig. 1c,d), though he was mechanically ventilated and could not sit or speak. He had no serious complications such as severe infections, cardiopulmonary dysfunction, scoliosis, or other neurological complications. Electroencephalography showed normal basic activities without paroxysmal discharges, and brain magnetic resonance image showed a mild myelination delay without structural abnormalities.

Muscle biopsy was obtained from the quadriceps at age 4 months. Specimens were immediately frozen and processed according to standard methods. The main pathological feature was nemaline bodies observed in the cytoplasm, but not in the nuclei (Fig. 3c); which were confirmed by electron microscopy (Fig. 4a,b). Additional features included very small type 1 fibers without central nuclei, fiber degeneration, or cellular infiltration (Fig. 3a, b, and d). Type 1 fibers were predominant, accounting for 71% of the total fiber number. Type 1 fibers were smaller than type 2 fibers by 34%, with the mean type 1 fiber diameter as $10.6 \pm 4.02\,\mu m$ (±SD) and with the mean type 2A fiber diameter as $16.1 \pm 5.17\,\mu m$ (±SD). Type 2B fibers were not detected, although there were a few Type 2C fibers. Neither the peripheral halo phenomenon nor central cores or minicores were observed (Fig. 3).

MATERIALS AND METHODS

Patients

The parents of the patient gave written informed consent for this study. The study was approved by the Ethics Committees of Tokyo Women's Medical University, Tokyo, Japan; and conformed to the guidelines involving human research as stated in the Declaration of Helsinki.

Targeted Capture and Next-Generation DNA Sequencing

Genomic DNA was extracted from peripheral blood leukocytes of the patient and his parents, using standard procedures. To identify disease-causing mutations, we used high-throughput screening system of congenital myopathies/muscular dystrophies-related genes through massively parallel sequencing with target gene capture, which we had established. The target gene capture was performed using the SureSelect™ Target Enrichment System (Agilent Technologies, CA). A custom set of SureSelect™ in-solution baits were designed using the eArray tool (http://www.opengenomics.com/earray) for capture of non-contiguous target muscle disease genomic regions approximately 3 Mb in total length, including *DMD* (OMIM 310200), *FKTN* (OMIM 607440), *LAMA2* (OMIM 156225), *DAG1* (OMIM 128239), *POMGNT1* (OMIM 606822), *POMT1* (OMIM 607423), *POMT2* (OMIM 607439), *TPM3, NEB, ACTA1, TPM2, TNNT1* (OMIM 191041),

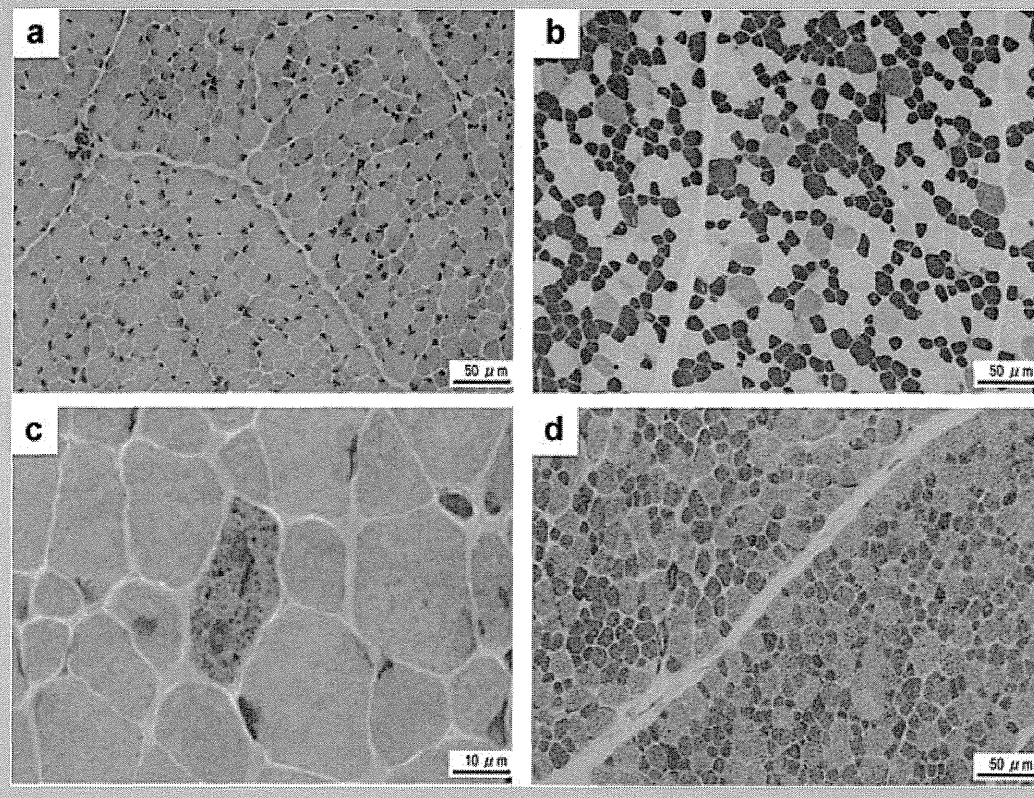

FIG. 3. Histopathological findings of skeletal muscle biopsy specimens. a: Hematoxylin–eosin staining showing fiber size variability without any dystrophic changes or inflammatory cell infiltrations. b: ATPase staining showing atrophic changes of type 1 fibers (dark stain) and decreased numbers of type 2B fibers (light stain). c: Modified Gomori trichrome staining showing nemaline bodies in the cytoplasm. d: NADH-TR staining showing type 1 fibers (dark stain) smaller than type 2 fibers (light stain). Bars indicate 50 μm (a, b, and d) or 10 μm (c).

CFL2 (OMIM 601443), *MTM1* (OMIM 300415), and *RYR1*. Then, 3 μg of the patient's genomic DNA was used for construction of a library composed of adaptor-ligated randomly fragmented DNA using the SOLiD Fragment Library Construction Kit (Applied Biosystems, CA) according to the manufacturer's instructions. The adaptor-ligated DNA was captured by hybridization in solution to the custom-designed cRNA oligonucleotide baits following the manufacturer's protocols. The enriched library DNA was sequenced using a SOLiD™ 4 System (Applied Biosystems) according to the manufacturer's instructions. The reads from each library were aligned against human genome sequence hg19 using Bioscope software (Applied Biosystems).

Validation of Mutations by Sanger Sequencing

For validation of detected variants, Sanger sequencing was performed. Primers were designed to amplify the detected novel missense mutations flanking sequence of *RYR1*. The amplification products were purified, directly sequenced with the BigDye terminator v3.1 Cycle Sequencing Kit (Applied Biosystems), and analyzed on a 3130×l genetic analyzer (Applied Biosystems).

RESULTS

More than 3,600 sequence variants were detected. Among them, we identified two non-synonymous single nucleotide substitutions in *RYR1*. These were heterozygous novel missense variants: c.4718 C > T (p.1573 Pro > Leu) in exon 33 and c.7585 G > A (p.2529 Asp > Asn) in exon 47. The nomenclature was based on the reference sequence *RYR1* (GenBank reference sequence, NM_000540.2), with nucleotide number 1 corresponding to the first base of the translation initiation codon. Sanger sequencing confirmed the variants and showed the parents to be heterozygous for each variant (Fig. 5). Neither of the variants was seen in 50 normal Japanese control samples, in 1000 Genomes Project data (http://www.1000genomes.org/data), or in the Exome Variant Server (EVS) Database (http://snp.gs.washington.edu/EVS/).

DISCUSSION

The patient we have described was clinically categorized into a severe congenital type of NM based on the clinical manifestations and histopathological findings, characterized by nemaline rods without central cores or minicores. Smallness of type 1 fibers, which is a non-specific common finding in many congenital

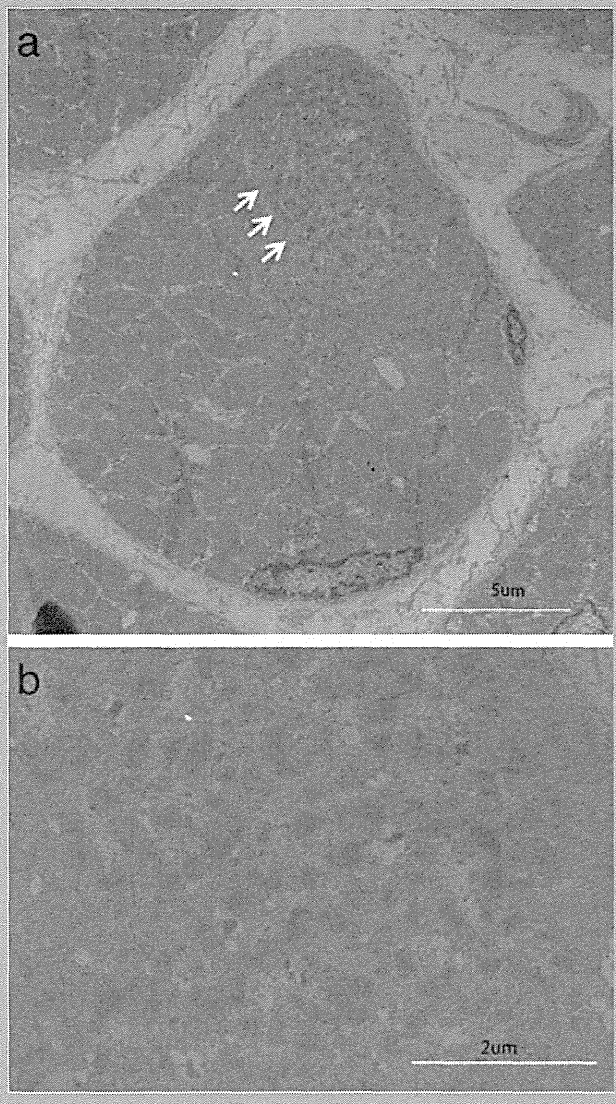

FIG. 4. Electron microscopic findings on the frozen quadriceps. Nemaline bodies were observed as numerous small rods in the cytoplasm (arrow). Bar indicates 5 μm (a) and 2 μm (b).

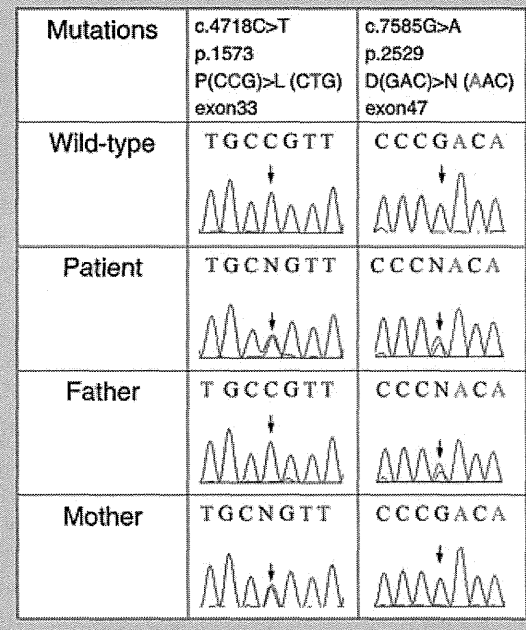

FIG. 5. Sanger sequencing of *RYR1*, showing compound heterozygous mutations: a C → T substitution (c.4718 C > T, p.1573 Pro > Leu) in exon 33 derived from his mother; a G → A substitution (c.7585 G > A, p.2529 Asp > Asn) in exon 47 derived from his father.

myopathies, does not take precedence over more specific findings such as nemaline rods [Clarke, 2011]. Massively parallel sequencing of congenital myopathy/muscular dystrophy-related genes has detected compound heterozygous missense *RYR1* variants, both of which are not found in the *RYR1* Locus-Specific Database in Leiden Open Variation Database (http://www.dmd.nl/nmdb2/home.php? select_db=RYR1) or in a comprehensive mutation review by Robinson et al. [2006]. There are two transcripts (NM_000540, NM_001042723) of *RYR1*. In NM_000540 including all exons of *RYR1*, PolyPhen-2 (Polymorphism Phenotyping v2, http://genetics.bwh.harvard.edu/pph2/) predicted p.1573 Pro > Leu as probably damaging with a score of 1 and p.2529 Asp > Asn Asn as benign with a score of 0.07; whereas in NM_001042723, a shorter isoform lacking an alternate in-frame exon, PolyPhen-2 predicted p.1573 Pro > Leu as benign with a score of 0.152 and p.2529 Asp > Asn as probably damaging with a score of 0.987 (See Supporting Information online Supplementary eTable I). SIFT (Sorting Intolerant From Tolerant; http://blocks.fhcrc.org/sift/SIFT.html) software packages predicted both variants in both transcripts as damaging (See Supporting Information online Supplementary eTable I). Moreover, phastCons and phyloP program (http://compgen.bscb.cornell.edu/phast) assessed proline at 1573 and aspartic acid at 2529 as highly conserved in human and other mammalian species (pig, rabbit, mouse) (See Supporting Information online Supplementary eTable I) and also in *RYR2* and *RYR3*, the genes encoding the other subtypes of the ryanodine receptor.

RYR1 encodes the principal sarcoplasmic reticulum Ca^{2+} release channel which plays a crucial role in excitation–contraction coupling [Zhou et al., 2007]. Dominant *RYR1* mutations are well-recognized causes of both malignant hyperthermia (MH) and central core disease (CCD) [Gillard et al., 1991; Quane et al., 1993; Zhang et al., 1993]. Recessive *RYR1* mutations have been identified in patients with CCD [Jungbluth et al., 2002; Kossugue et al., 2007], in those with CCD, transiently presenting as multi-minicore disease [Ferreiro et al., 2002], in those with minicore myopathy with external ophthalmoplegia [Monnier et al., 2003; Jungbluth et al., 2005; Monnier et al., 2008; Wilmshurst et al., 2010], and in those with congenital fiber type disproportion (CFTD) frequently with ophthalmoplegia [Clarke et al., 2010]. Severe CCD patients presenting with fetal akinesia were associated with dominant and recessive *RYR1* mutations [Romero et al., 2003].

Both cores and nemaline rods were observed in patients with CCD associated with heterozygous *RYR1* mutations [Monnier et al., 2000; Scacheri et al., 2000]. *RYR1* mutations could cause several types of congenital myopathies with various severities including fetal akinesia and with ophthalmoplegia frequently, which would be consistent with clinical and pathological features of the present patient. We, therefore, concluded that the *RYR1* mutations identified in this study were pathogenic. The difference from previous patients with *RYR1* mutations is the lack of central cores or minicores and the presence of nemaline bodies, which allows the diagnosis as NM.

Zhou et al. [2007] reported that most dominant *RYR1* mutations, associated with a CCD phenotype and prominent cores, occurred mainly in the *RYR1* C-terminal exons 101 and 102. In contrast, recessive *RYR1* mutations were distributed evenly along the entire gene with variable expressivity: clinically, ranging from a typical CCD phenotype to generalized muscle weakness and wasting with external ophthalmoplegia as well as bulbar involvement and respiratory impairment; histopathologically, CFTD, central nuclei, and CCD. Indeed, the novel compound heterozygous *RYR1* mutations in exons 33 and 47 in the present patient caused various clinical features including fetal akinesia, neonatal severe muscle weakness/hypotonia, resipiratory insufficiency, persistent ophthalmoplegia, and an improving clinical course. Furthermore, several different *RYR1* mutations associated with recessive congenital myopathy and dominant MH in the same family have been reported [Zhou et al., 2007; Carpenter et al., 2009]. The novel missense mutations found in the present patient might confer susceptibility to MH in heterozygous mutation carriers in the family, despite no family history of MH, which could be useful information to recommend that the patient and his parents should be tested for MH susceptibility.

Congenital myopathies are a clinically, histopathologically, and molecularly heterogeneous group of disorders defined by hypotonia and muscle weakness, that usually present at birth or early infancy, in association with characteristic histopathological changes in skeletal muscle. Disease-causing genes of many congenital myopathies have been uncovered, but determining pathogenic mutation(s) in each patient is complicated [Sewry, 2008]. Firstly, there are substantial clinical and molecular overlaps among each type. Secondly, standard Sanger sequencing-based genetic screening for targeted genes corresponding to clinical diagnosis is expensive, time-consuming, and laborious. Recent advances in sequencing technologies have dramatically increased the speed and efficiency of DNA testing. In particular, the enrichment technique of target gene capture followed by massively parallel "next-generation" sequencing now allows more comprehensive and high-throughput genetic screening on several conditions with significant genetic heterogeneity such as cancer-predisposing disorders [Walsh et al., 2010], non-syndromic hearing loss [Shearer et al., 2010], ataxia [Hoischen et al., 2010], and retinitis pigmentosa [Simpson et al., 2011]. Identification of recessive *RYR1* mutations in the present patient suggests that congenital myopathies would be a good candidate for massively parallel sequencing-based genetic screening.

In conclusion, this is the first report of *RYR1* mutations in a patient clinically diagnosed with NM. He had severe perinatal manifestations with fetal akinesia and nemaline bodies in muscle histology, typical of severe congenital NM. He also had persistent ophthalmoplegia and histopathologically small type 1 fibers, but without central cores or minicores. We suggest that congenital myopathies, a clinically, histopathologically, and molecularly heterogeneous group of disorders are a good candidate for massively parallel sequencing-based genetic screening. Gene-based delineation through this innovative technology might solve clinical and histological confusion in congenital myopathies.

ACKNOWLEDGMENTS

The authors are grateful to the patient and his parents. We also wish to thank Dr. Haruko Suzuki for her kind advice on the histopathological analysis and Dr. Keiko Shishikura for her critical comments on the electron microscopic investigation. This work was supported by Grants-in-Aid from the Research Committee of Spinal muscular atrophy (SMA) (K.S.), funds from the Support Center for Women's Health Care Professionals and Researchers (E.K., K.S.), Research on Intractable Diseases, Ministry of Health, Labour and Welfare, Japan (T.K., K.S.); and Ministry of Education, Culture, Sports, Science and Technology in Japan (T.F., K.S.).

REFERENCES

Agrawal PB, Strickland CD, Midgett C, Morales A, Newburger DE, Poulos MA, Tomczak KK, Ryan MM, Iannaccone ST, Crawford TO, Laing NG, Beggs AH. 2004. Heterogeneity of nemaline myopathy cases with skeletal muscle alpha-actin gene mutations. Ann Neurol 56:86–96.

Carpenter D, Ismail A, Robinson RL, Ringrose C, Booms P, Iles DE, Halsall PJ, Steele D, Shaw MA, Hopkins PM. 2009. A *RYR1* muation associated with recessive congenital myopathy and dominant malignant hyperthermia in asian families. Muscle Nerve 40:633–639.

Clarke NF. 2011. Annotation. Congenital fibre type disproportion—A syndrome at the crossroads of the congenital myopathies. Neuromuscul Disord 21:252–253.

Clarke NF, Waddell LB, Cooper ST, Perry M, Smith RL, Kornberg AJ, Muntoni F, Lillis S, Straub V, Bushby K, Guglieri M, King MD, Farrell MA, Marty I, Lunardi J, Monnier N, North KN. 2010. Recessive mutations in *RYR1* are a common cause of congenital fiber type disproportion. Hum Mutat 31:E1544–E1550.

Ferreiro A, Monnier N, Romero NB, Leroy JP, Bönnemann C, Haenggeli CA, Straub V, Voss WD, Nivoche Y, Jungbluth H, Lemainque A, Volt T, Lunardi J, Fardeau M, Guicheney P. 2002. A recessive form of central core disease, transiently presenting as multi-minicore disease, is associated with a homozygous mutation in the ryanodine receptor type 1 gene. Ann Neurol 51:750–759.

Gillard EF, Otsu K, Fujii J, Khanna VK, de Leon S, Derdemezi J, Britt BA, Duff CL, Worton RG, MacLennan DH. 1991. A substitution of cysteine for arginine 614 in the ryanodine receptor is potentially causative of human malignant hyperthermia. Genomics 11:751–755.

Hoischen A, Gilissen C, Arts P, Wieskamp N, van der Vliet W, Vermeer S, Steehouwer M, de Vries P, Meijer R, Seiqueros J, Knoers NV, Buckley MF, Scheffer H, Veltman JA. 2010. Massively parallel sequencing of ataxia genes after array-based enrichment. Hum Mutat 31:494–499.

Jungbluth H, Müller CR, Halliger-Keller B, Brockington M, Brown SC, Feng L, Chattopadhyay A, Mercuri E, Manzur AY, Ferreiro A, Laing NG, Davis MR, Roper HP, Dubowitz V, Bydder G, Sewry CA, Muntoni F.

2002. Autosomal recessive inheritance of *RYR1* mutations in a congenital myopathy with cores. Neurology 59:284–287.

Jungbluth H, Zhou H, Hartley L, Halliger-Keller B, Messina S, Longman C, Brockington M, Robb SA, Straub V, Voit T, Swash M, Ferreiro A, Bydder G, Sewry CA, Müller C, Muntoni F. 2005. Minicore myopathy with ophthalmoplegia caused by mutations in the ryanodine receptor type 1 gene. Neurology 65:1930–1935.

Kossugue PM, Paim JF, Navarro MM, Silva HC, Pavanello RCM, Gurgel-Giannetti J, Zatz M, Vainzof M. 2007. Central core disease due to recessive mutations in *RYR1* gene: Is it more common than described? Muscle Nerve 35:670–674.

Monnier N, Romero NB, Lerale J, Nivoche Y, Qi D, MacLennan DH, Fardeau M, Lunardi J. 2000. An autosomal dominant congenital myopathy with cores and rods is associated with a neomutation in the *RYR1* gene encoding the skeletal muscle ryanodine receptor. Hum Mol Genet 9:2599–2608.

Monnier N, Ferreiro A, Marty I, Labarre-Vila A, Mezin P, Lunardi J. 2003. A homozygous splicing mutation causing a depletion of skeletal muscle RYR1 is associated with multi-minicore disease congenital myopathy with ophthalmoplegia. Hum Mol Genet 12:1171–1178.

Monnier N, Marty I, Faure J, Castiglioni C, Desnuelle C, Sacconi S, Estournet B, Ferreiro A, Romero N, Laquerriere A, Lazaro L, Martin JJ, Morava E, Rossi A, Van der Kooi A, de Visser M, Verschuuren C, Lunardi J. 2008. Null mutations causing depletion of the type 1 ryanodine receptor (RYR1) are commonly associated with recessive structural congenital myopathies with cores. Hum Mutat 29:670–678.

North K, Ryan MM. 2010. Nemaline myopathy. In: GeneReviews at genetests: Medical Genetics Information Resource (database online). Copyright, University of Washington, Seattle, 1997–2011. Available at http://www.genetests.org. Accessed May 14, 2011.

Quane KA, Healy JMS, Keating KE, Manning BM, Couch FJ, Palmucci LM, Doriguzzi C, Fagerlund TH, Berg K, Ording H, Bendlxen D, Mortier W, Linz U, Muller CR, McCarthy TV. 1993. Mutations in the ryanodine receptor gene in central core disease and malignant hyperthermia. Nat Genet 5:51–55.

Robinson R, Carpenter D, Shaw MA, Halsall J, Hopkins P. 2006. Mutations in *RYR1* in malignant hyperthermia and central core disease. Hum Mutat 27:977–989.

Romero NB, Monnier N, Viollet L, Cortey A, Chevallay M, Leroy JP, Lunardi J, Fardeau M. 2003. Dominant and recessive central core disease associated with *RYR1* mutations and fetal akinesia. Brain 126: 2341–2349.

Scacheri PC, Hoffman EP, Fratkin JD, Semino-Mora C, Senchak A, Davis MR, Laing NG, Vedanarayanan V, Subramony SH. 2000. A novel ryanodine receptor gene mutation causing both cores and rods in congenital myopathy. Neurology 55:1689–1696.

Sewry CA. 2008. Pathological defects in congenital myopathies. J Muscle Res Cell Motil 29:231–238.

Shearer AE, Deluca AP, Hildebrand MS, Taylor KR, Gurrola J II, Sherer S, Scheetz TE, Smith RJH. 2010. Comprehensive genetic testing for hereditary hearing loss using massively parallel sequencing. Proc Natl Acad Sci 107:21104–21109.

Simpson DA, Clark GR, Alexander S, Silvestri G, Willoughby CE. 2011. Molecular diagnosis for heterogeneous genetic diseases with targaet high-throughput DNA sequencing applied to retinitis pigmentosa. J Med Genet 48:145–151.

Walsh T, Lee MK, Casadei S, Thornton AM, Stray SM, Pennil C, Nord AS, Mandell JB, Swisher EM, King MC. 2010. Detection of inherited mutations for breast and ovarian cancer using genomic capture and massively parallel sequencing. Proc Natl Acad Sci 107:21104–21109.

Wilmshurst JM, Lillis S, Zhou H, Pillay K, Henderson H, Kress W, Müller CR, Ndondo A, Cloke V, Cullup T, Bertini E, Boennemann C, Straub V, Quinlivan R, Dowling JJ, Al-Sarraj S, Treves S, Abbs S, Manzur AY, Sewry CA, Muntoni F, Jungbluth H. 2010. *RYR1* mutations are a common cause of congenital myopathies with central nuclei. Ann Neurol 68:717–726.

Zhang Y, Chen HS, Khanna VK, De Leon S, Phillips MS, Schappert K, Britt BA, Browell AK, MacLennan DH. 1993. A mutation in the human ryanodine receptor gene associated with central core disease. Nat Genet 5:46–50.

Zhou H, Jungbluth H, Sewry CA, Feng L, Bertini E, Bushby K, Straub V, Roper H, Rose MR, Brockington M, Kinali M, Manzur A, Robb S, Appleton R, Messina S, D'Amico A, Quinlivan R, Swash M, Müller CR, Brown S, Treves S, Muntoni F. 2007. Molecular mechanisms and phenotypic variation in *RYR1*-related congenital myopathies. Brain 130:2024–2036.

Cell Tissue Res (2012) 348:189–197
DOI 10.1007/s00441-012-1340-9

REGULAR ARTICLE

Human first-trimester chorionic villi have a myogenic potential

Reiko Arakawa · Ryoko Aoki · Masayuki Arakawa · Kayoko Saito

Received: 27 June 2011 / Accepted: 18 January 2012 / Published online: 28 February 2012

Abstract First-trimester chorionic-villi-derived cells (FTCVs) are the earliest fetal material that can be obtained for prenatal diagnosis of fetal disorders such as Duchenne muscular dystrophy (DMD). DMD is a devastating X-linked disorder characterized by the absence of dystrophin at the sarcolemma of muscle fibers. Currently, a limited number of treatment options are available for DMD, although cell therapy is a promising treatment strategy for muscle degeneration in DMD patients. A novel candidate source of cells for this approach is FTCVs taken between the 9th and 11th weeks of gestation. FTCVs might have a higher undifferentiated potential than any other tissue-derived cells because they are the earliest fetal material. We examined the expression of mesenchymal stem cell and pluripotent stem cell markers in FTCVs, in addition to their myogenic potential. FTCVs expressed mesenchymal stem cell markers and *Nanog* and *Sox2* transcription factors as pluripotent stem cell markers. These cells efficiently differentiated into myotubes after myogenic induction, at which point *Nanog* and *Sox2* were down-regulated, whereas *MyoD*, *myogenin*, *desmin* and *dystrophin* were up-regulated. To our knowledge, this is the first demonstration that FTCVs can be efficiently directed to differentiate in vitro into skeletal muscle cells that express dystrophin as the last stage marker of myogenic differentiation. The myogenic potential of FTCVs reveals their promise for use in cell therapy for DMD, for which no effective treatment presently exists.

Keywords Duchenne muscular dystrophy · First-trimester chorionic villi · Myogenic differentiation · Dystrophin · Cell therapy

Electronic supplementary material The online version of this article (doi:10.1007/s00441-012-1340-9) contains supplementary material, which is available to authorized users.

This work was supported by a Research Grant (20B-13-03) for Nervous and Mental Disorders from the Ministry of Health, Labour and Welfare; Grants-in-Aid from the Research Committee of Spinal Muscular Atrophy (SMA) from the Ministry of Health, Labour and Welfare of Japan; and the Global COE program, Multidisciplinary Education and Research Center for Regenerative Medicine (MERCREM) from the Ministry of Education, Culture, Sports Science, and Technology (MEXT), Japan.

R. Arakawa · K. Saito
Affiliated Field of Medical Genetics, Division of Biomedical Engineering and Science, Graduate Course of Medicine, Graduate School of Tokyo Women's Medical University, 10-22 Kawadacho, Shinjyuku, Tokyo 162-0054, Japan

R. Arakawa · R. Aoki · K. Saito (✉)
Institute of Medical Genetics, Tokyo Women's Medical University, 10-22 Kawadacho, Shinjyuku, Tokyo 162-0054, Japan
e-mail: saito@img.twmu.ac.jp

M. Arakawa
Institute of Microbial Chemistry, Microbial Chemistry Research Foundation, 3-14-23 Kamiosaki, Shinagawa, Tokyo 141-0021, Japan

Introduction

In the early 1980s, prenatal diagnosis by using chorionic villus sampling (CVS) was introduced; this method has advanced the diagnosis of fetal genetic disorders such as Duchenne muscular dystrophy (DMD) in the first-trimester of pregnancy. The numerous advances in prenatal diagnosis and molecular genetic testing of DMD have permitted the accurate and early diagnosis of carrier women.

During human development, the morula constitutes the inner cell mass and the outer cell mass. The outer cell mass forms the trophoblasts, which later contribute to the formation

of the placenta. In the early weeks of development, villi derived from the trophoblasts give rise to the chorionic villi (Sadler 2009). The first-trimester chorionic villi can be collected for CVS. By the third trimester of pregnancy, the placenta consists in two components: a fetal portion, which is derived from the chorionic villus, the smooth chorion, the chorionic plate and the amnion and a maternal portion.

Of note, the first-trimester chorionic-villi-derived cells (FTCVs) are the earliest fetal material that can be obtained during pregnancy. Despite the presence of stem cells in the FTCV population, only a few detailed reports have been presented on the differentiation capability of fetal cells obtained from CVS (Poloni et al. 2008; Spitalieri et al. 2009). Furthermore, third-trimester placental chorionic-villi-derived cells (TTCVs) are either myogenic progenitors or have myogenic potential (Kawamichi et al. 2010).

DMD is the most common and severe form of muscular dystrophy. DMD is an X-linked recessive genetic disease that affects 1 in 3,500 newborn male children and is caused by a deficiency in dystrophin, which is associated with a large oligomeric complex of glycoproteins that link the cytoskeleton to the extracellular matrix (Ervasti and Campbell 1991). The absence of dystrophin results in the destabilization of the architecture of the extracellular membrane/sarcolemma cytoskeleton, making muscle fibers susceptible to contraction-associated mechanical stress and degeneration.

Unfortunately, no curative therapy is available for DMD, although a few novel treatments, including pharmacologic agents and genetic alterations for replacing the missing dystrophin by exon skipping or viral gene delivery, are in clinical trials (Kinali et al. 2009; Miyagoe-Suzuki and Takeda 2010). Another attractive alternative for treating DMD is cell therapy for every gene mutation in patients. In particular, myoblasts are the first choice as cellular therapeutics for skeletal muscle, because of their intrinsic myogenic commitment (Grounds et al. 2002). However, myoblasts recovered from muscle biopsies are known to be poorly expandable in vitro and rapidly senesce (Cossu and Mavilio 2000). Therefore, an alternative source of muscle progenitor cells is desirable. Accordingly, researchers have become interested in a variety of other cells with myogenic potential, including bone marrow stromal cells (Saburina et al. 2004), blood-vessel-associated mesoangioblasts (Sampaolesi et al. 2006), umbilical cord blood cells (Gang et al. 2004), adipose tissue cells (Di Rocco et al. 2006), endometrial and menstrual blood cells (Cui et al. 2007), placenta cells (Kawamichi et al. 2010) and induced pluripotent stem cells from DMD (Kazuki et al. 2010).

In this study, we have identified a subpopulation of cells that express various markers of mesenchymal stem cells (MSCs) and pluripotent stem cells in the larger FTCV population. Subsequently, we have found that directed differentiation of the FTCVs into skeletal muscle cells in vitro efficiently generates dystrophin-positive myotubes.

Materials and methods

Isolation of first-trimester chorionic villi and placental tissues

First-trimester chorionic villi were excised from subjects undergoing prenatal diagnosis between the 9th and 11th weeks of gestation. Each biopsy was performed by using standard procedures under continuous ultrasound guidance. The human placentas were collected between the 37th and 41st weeks of gestation (third trimester) during normal full-term deliveries. For this study, the first-trimester chorionic villi were obtained from 12 individuals and placentas were obtained from five individuals. Of note, the cells from both these sources are established as having the normal full-length *dystrophin* gene without any mutations. Informed patient consent was obtained in all cases. Ethical approval for tissue collection was granted by the Institutional Review Board of Tokyo Women's Medical University, Japan.

Tissue and cell culture

All the first-trimester chorionic villi and placentas were processed within 24 h of collection. After the villi had been cut into small pieces, the tissues were cultured in AmnioMAX-C100 medium (Invitrogen, Carlsbad, Calif., USA), whereas the placentas were washed extensively with phosphate-buffered saline (PBS). Once the amnion had been peeled off, each placenta was separated into three parts, namely, the chorionic villus, chorionic plate and decidua basalis. To isolate TTCVs, placental chorionic villi were subsequently minced by using scissors and re-suspended in MSC basal medium (Lonza, Walkersville, Md., USA). The FTCVs and TTCVs were maintained separately at 37°C in a humidified atmosphere containing 5% CO_2 and were allowed to attach to their culture vessels. After cells had attached to their vessels, the medium was regularly changed twice a week. Once the cells had grown to 70%–80% confluence, they were harvested with trypsin (0.25%) and 1 mM EDTA (0.02%) in PBS (1:1 v/v) and were subsequently plated onto new dishes. After the second passage, FTCVs were cultured in MSC basal medium.

The pluripotent human embryonal carcinoma cell line NTERA-2 clone D1 was purchased from the European Collection of Cell Cultures (Porton Down, Salisbury, UK). Normal human dermal fibroblasts (HDFs) were purchased from Lonza. NTERA-2 and HDFs were cultured in Dulbecco's modified Eagle's medium (DMEM) supplemented with 10% fetal bovine serum (FBS) and 2 mM glutamine.

Flow cytometric analysis

FTCVs and TTCVs obtained between the third and sixth passages of culture were characterized by flow cytometric

analysis. Antibodies against human CD29, CD34, CD44, CD73 and CD105 were purchased from Beckman Coulter (Brea, Calif., USA) and BD Biosciences Pharmingen (San Diego, Calif., USA). Briefly, the cells were stained with primary antibodies and fluorescently labeled secondary antibodies, each for 20 min at 4°C. The cells were then assessed on an EPICS XL-MCL analyzer (Beckman Coulter). Three independent experiments were performed in triplicate.

Quantitative analysis by real-time and semi-quantitative reverse transcription with polymerase chain reaction

Total RNA was prepared by using TRIzol Reagent (Invitrogen). Human skeletal muscle total RNA was purchased from Clontech Laboratories (Mountain View, Calif., USA). An aliquot of 0.1–2 μg total RNA was reverse-transcribed into cDNA with SuperScript III Reverse Transcriptase (Invitrogen) according to the manufacturer's protocol.

For quantitative real-time reverse transcription (RT) with polymerase chain reaction (PCR) analysis (qPCR), PCR was performed by using a Fast Start Universal SYBR Green Master (ROX) kit (Roche Diagnostics, Mannheim, Germany) and the Applied Biosystems 7500 Real-Time PCR System (Applied Biosystems, Foster City, Calif., USA). Relative expression levels were calculated by using the $\Delta\Delta C_T$ method after normalization to the housekeeping gene *GAPDH* (*D-glyceraldehyde-3-phosphate dehydrogenase*).

Semi-quantitative RT-PCR analysis was performed with TaKaRa ExTaq (TaKaRa Bio, Shiga, Japan) for 30 cycles, with each cycle consisting in 94°C for 30 s, 65°C for 30 s and 72°C for 20 s, followed by an additional 10 min incubation at 72°C after completion of the last cycle. The transcript level of the *dystrophin* gene was standardized to the ribosomal RNA *18S* gene level. The primer sequences used for qPCR and RT-PCR are listed in Supplementary Table 1. For each experiment, at least two independent qPCR and RT-PCR experiments were performed.

In vitro myogenesis

The method used herein for in vitro myogenesis was modified as previously described (Kawamichi et al. 2010). FTCVs obtained between the second and fifth passages of culture were seeded at a density of 3×10^4 cells/ml in growth medium (DMEM supplemented with 20% FBS) onto 60-mm collagen-I-coated cell culture dishes (Asahi Glass, Tokyo, Japan). At 48 h after being seeded onto the collagen I-coated dishes, the cells were treated with 5 μM 5-azacytidine (Sigma-Aldrich, St. Louis, Mo., USA) for 24 h. Cell culture was then maintained in differentiation medium (DMEM supplemented with 2% horse serum) for 21 days. The differentiation medium was changed twice a week until the experiment was terminated.

Dystrophin and myosin heavy chain expression by immunocytochemistry

The FTCVs obtained before 5-azacytidine treatment and 21 days after treatment were rinsed twice with PBS, fixed with 4% paraformaldehyde in PBS at room temperature for 20 min, permeabilized with cold 100% methanol on ice for 10 min and subsequently rinsed with PBS (3×5 min). The cells were treated with PBS containing 10% horse serum at room temperature for 45 min and were then incubated with rabbit polyclonal anti-dystrophin antibody (Abcam, Cambridge, UK) diluted 1:100 with mouse monoclonal anti-sarcomeric myosin heavy chain protein (MF20; Developmental Studies Hybridoma Bank, University of Iowa) overnight at 4°C. The cells were then washed three times with PBS for 10 min and incubated with secondary antibodies (goat anti-rabbit IgG [H+L] Alexa Fluor 488 and goat anti-mouse IgG [H+L] Alexa Fluor 594 conjugate; Molecular Probes, Eugene, Ore., USA), which were diluted 1:400 with PBS containing 2% bovine serum albumin, for 30 min at room temperature. After this incubation, the cells were washed with PBS three times, treated with Hoechst dye (0.1 μg/ml) at room temperature for 10 min, washed with PBS once, observed under a fluorescence microscope (ECLIPSE TE2000-U; Nikon, Tokyo, Japan) and then photographed by using an AxioCam HRC (Carl Zeiss MicroImaging, Tokyo, Japan). All micrographs were taken under identical conditions with the same exposure time. Three independent experiments were performed in triplicate. The fusion index was determined by calculating the percentage of nuclei in MF20-positive (MF20+) myotubes in five randomly encountered fields (a magnification of ×200 per field) per well in triplicate wells.

Pluripotent marker expression by immunocytochemistry

The FTCVs obtained before 5-azacytidine treatment and 1 day after treatment were rinsed twice with PBS, fixed with 4% paraformaldehyde in PBS at room temperature for 20 min and permeabilized with 0.1% Triton X-100 in PBS for 10 min and subsequently rinsed with PBS (3×5 min). The cells were treated with PBS containing 10% goat serum at room temperature for 45 min and were then incubated with primary antibodies (rabbit monoclonal anti-Nanog, Oct4, Sox2 antibody; Cell Signaling Technology, Danvers, Mass., USA) diluted 1:400 with 10% goat serum in PBS overnight at 4°C. Then, the cells were washed three times with PBS for 10 min and incubated with secondary antibodies (goat anti-rabbit IgG [H+L] Alexa Fluor 488 and goat anti-mouse IgG [H+L] Alexa Fluor 594 conjugate; Molecular Probes), which were diluted 1:400 with PBS containing 2% bovine serum albumin, for 30 min at room temperature. After this incubation, the cells were washed with PBS three times, treated with Hoechst dye

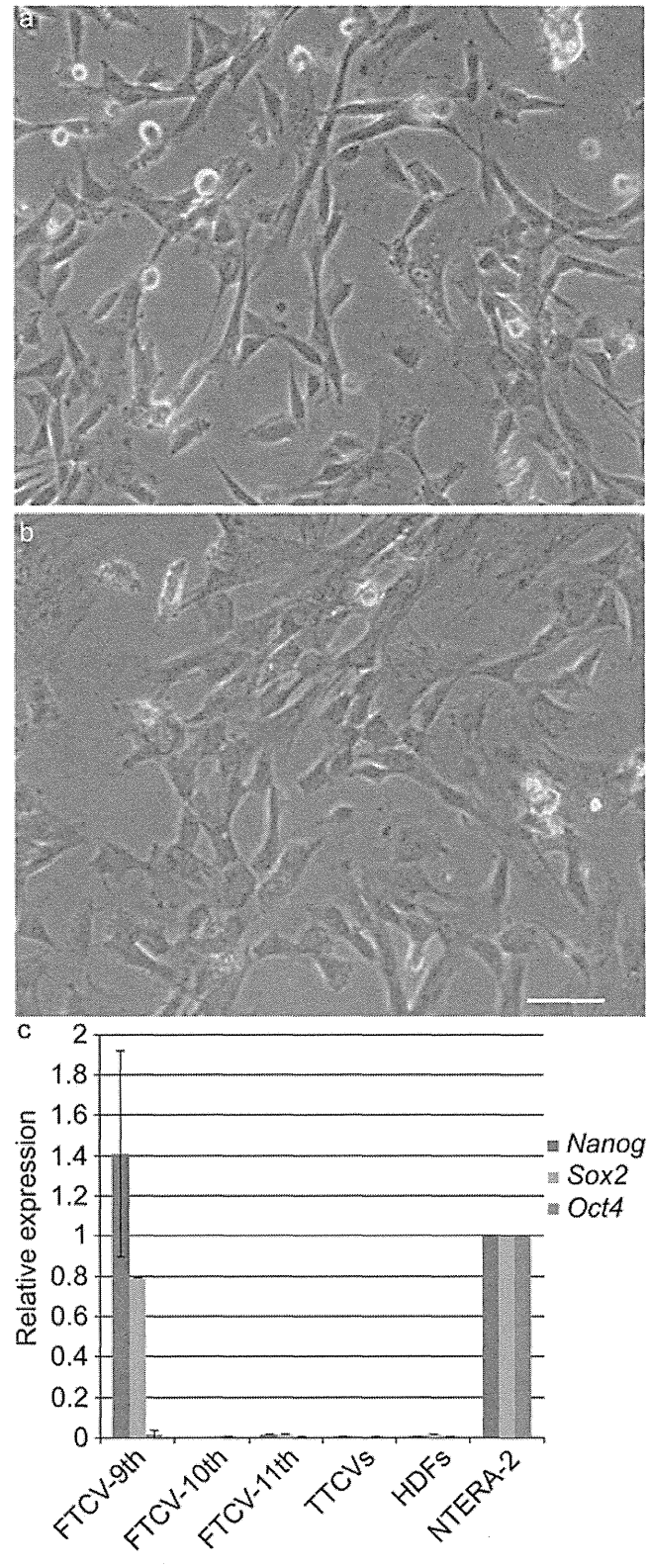

Fig. 1 Phase contrast microscopic images of undifferentiated first-trimester chorionic-villi-derived cells (FTCVs; **a**) and third-trimester placental chorionic-villi-derived cells (TTCVs; **b**). *Bar* 50 μm. **c** Quantitative real-time reverse transcription with polymerase chain reaction (qPCR) analysis for *Nanog*, *Sox2* and *Oct4* mRNA expression in FTCVs at the 9th (FTCV-9th), 10th (FTCV-10th) and 11th (FTCV-11th) weeks of gestation, TTCVs, normal human dermal fibroblasts (HDFs) and a pluripotent human embryonic carcinoma cell line (NTERA-2). The value for NTERA-2 was set to 1 in each experiment. Each value (n=4) represents the mean±SD

at room temperature for 10 min, washed with PBS once and then observed under a fluorescence microscope.

Western blotting

The FTCVs obtained before 5-azacytidine treatment and 21 days after treatment on 60-mm collagen-I-coated dishes were scraped in 1 ml homogenizing buffer consisting in 0.02 mol/l NaOH, 1% sodium dodecyl sulfate (SDS, Sigma-Aldrich), 5 mM O,O′-Bis [2-aminoethyl] ethyleneglycol-N, N, N′, N′-tetraacetic acid (Dojindo Molecular Technologies, Kumamoto, Japan) and Complete Mini (Roche Diagnostics), on ice and the cells were collected. Homogenates were collected in separate microcentrifuge tubes and centrifuged at 15,000*g* for 30 min at 4°C. Equal amounts of protein (10 μg) were loaded onto SDS-polyacrylamide gels and blotted onto Immobilon-P membranes (Millipore, Bedford, Mass., USA) by using a semi-dry transfer system (Atto, Tokyo, Japan). The blots were incubated with primary antibodies against dystrophin (NCL-DYS2 [1:200] and NCL-DYS3 [1:50; Novocastra Laboratories, Newcastle upon Tyne, UK]) for 3 h at room temperature and were subsequently washed three times with blocking buffer. The blots were then incubated with a peroxidase-conjugated goat anti-mouse IgG (H+L) secondary antibody (0.05 μl/ml; Jackson ImmunoResearch Laboratories, West Grove, Pa., USA; directed against the primary antibody) for 2 h at room temperature. The membranes were subsequently treated with an enzyme chemiluminescence assay (ECL plus Western Blotting Detection System; GE Healthcare, Buckinghamshire, UK) and the reactions were visualized by exposing the membranes to an X-ray film (Hyperfilm ECL; GE Healthcare) overnight.

Results

Expression of mesenchymal stem cell markers in undifferentiated FTCVs and TTCVs

We successfully cultured a large number of primary cells from FTCVs and TTCVs and found that these cells showed a fibroblast-like morphology at the second passage of culture (Fig. 1a, b). After isolation of the cells, we immunocytochemically evaluated the expression of the surface markers present on the uninduced FTCVs and TTCVs from three individuals by flow cytometry (Table 1). Both FTCVs and TTCVs were positive for MSC markers CD29, CD44, CD73 and CD105 but were negative for the CD34 hematopoietic marker, indicating that both the FTCV- and TTCV-cultured populations